Published in final edited form as:
Curr Probl Cardiol. 2010 April ; 35(4): 176–220. doi:10.1016/j.cpcardiol.2009.12.002.

Cardiovascular Magnetic Resonance Imaging of Myocardial Infarction, Viability, and Cardiomyopathies

Amy M. West, MD[a] and **Christopher M. Kramer, MD**[b]

[a]Fellow Physician, Division of Cardiovascular Medicine, University of Virginia, Charlottesville, Virginia

[b]Professor of Medicine and Radiology, Director, Cardiovascular Imaging Center, University of Virginia, Charlottesville, Virginia

Abstract

Cardiovascular magnetic resonance provides the opportunity for a truly comprehensive evaluation of patients with a history of MI, with regards to characterizing the extent of disease, impact on LV function and degree of viable myocardium. The use of contrast-enhanced CMR for first-pass perfusion and late gadolinium enhancement is a powerful technique for delineating areas of myocardial ischemia and infarction. Using a combination of T2-weighted and contrast-enhanced CMR images, information about the acuity of an infarct can be obtained. There is an extensive amount of literature using contrast-enhanced CMR to predict myocardial functional recovery with revascularization in patients with ischemic cardiomyopathies. In addition, CMR imaging in patients with cardiomyopathies can distinguish between ischemic and non-ischemic etiologies, with the ability to further characterize the underlying pathology for non-ischemic cardiomyopathies.

Keywords

Cardiovascular magnetic resonance; cardiac imaging; CMR; cardiomyopathy; viability

Introduction

Patient prognosis after an acute myocardial infarction (MI) is influenced by left ventricular (LV) function, infarct size, the status of microvasculature within the infarct zone, the amount of salvaged myocardium after reperfusion, as well as additional clinical characteristics. As a result, patient risk stratification after an acute MI often includes a multi-modality imaging approach with echocardiography, ventriculography, and/or cardiac magnetic resonance imaging (CMR). CMR has the unique ability to assess global and regional LVfunction post-MI, quantify infarct size with late gadolinium enhancement, assess

Corresponding author for proof and reprints: Christopher M. Kramer, MD, University of Virginia Health System, Departments of Medicine and Radiology, Lee Street, Box 800170, Charlottesville, VA 22908, ckramer@virginia.edu Telephone: (434) 243-0736, Fax: (434) 982-1998.

Disclosure statement: Christopher M. Kramer MD: Consultant and research support: Siemens Medical Solutions, Research grant: Astellas

the status of the microvasculature by identifying microvascular obstruction (MO, and evaluate the area at risk with T2-weighted imaging of myocardial edema. (1) Thus, CMR is uniquely positioned to comprehensively evaluate the post-infarct patient. A multi-center international clinical trial is being planned to compare the prognostic capabilities of CMR and echocardiography in the prediction of death and other cardiovascular outcome measures in acute MI. The underlying hypothesis is that the comprehensive evaluation of the myocardium enabled with CMR will increase the power of imaging to predict events.

In addition, CMR plays an important role in assessing patients prior to revascularization. In chronic MI CMR evaluation of the transmurality of infarction relates to the likelihood of functional recovery of dysfunctional myocardium. Contractile reserve in response to dobutamine is an accurate measure of viability as well. The two approaches, anatomic and physiologic, can be used together to improve the accuracy of viability assessment.

Late gadolinium enhancement plays an important role in the assessment of patients with congestive heart failure and cardiomyopathies. Certain patterns of late gadolinium enhancement are associated with particular cardiomyopathies. This manuscript will review the use of CMR in the comprehensive evaluation of patients with MI chronic ischemic heart disease prior to revascularization, and cardiomyopathies.

1. Comprehensive Assessment of Myocardial Infarction with CMR

1.a Left Ventricular Function and Segmental Wall Motion Abnormalities

Evaluation of LV systolic function and segmental wall motional abnormalities in a coronary distribution after an acute MI is readily performed by CMR. Analysis of LV function with CMR uses cine steady state free precession images to obtain 2-chamber, 3-chamber, 4-chamber long axis views of the left ventricle. A stack of sequential short axis images of the left ventricle beginning at the base through the apex are obtained and analyzed using the American Heart Association (AHA) 17-segment model. (2) Wall thickening can be qualitatively graded as follows: normal, mild-moderate hypokinesis, severe hypokinesis, akinesis and dyskinesis.

CMR is inherently quantitative. Sequential short axis images are used to calculate a LV ejection fraction (EF) based on the difference between the sum of the endocardial LV contoured areas at end-diastole and end-systole. Holman et al used gradient echo imaging at sequential short axis slices covering the entire heart in 25 patients within three weeks of first anterior MI and in a control group of almost fifty healthy volunteers. (3) Analysis of the short axis images for regional wall motion abnormalities required endocardial and epicardial countours drawn manually and a centerline method was used to calculate wall thickness at end-diastole and end-systole. Patients with anterior MI demonstrated relative thinning of the myocardium at end-diastole and reduced wall thickening at end-systole. The authors found that patients post-MI had a significantly lower systolic wall thickening for segments supplied by the left anterior descending artery compared to normal volunteers. In addition to wall thickening, another method for evaluating regional wall motion abnormalities measures regional myocardial strain by using grid-tagging with spatial modulation of magnetization. (4) In the study by Gotte et al, patients post-MI had regional wall thickening compared to regional wall strain as assessed by using groups of three tagging intersection points to create triangular myocardial elements which could be deformed in radial or circumferential directions during the cardiac cycle. In the infarct group, patients had a significantly lower regional wall thickening in all areas of the left ventricle, including the infarct-related area as well as the adjacent and remote myocardium. The strain analysis with myocardial tagging in patients post infarction demonstrated a significant difference in contractile function in infarct-related and remote myocardium whereas wall thickening did not.

CMR has been validated against echocardiography for measuring LV volumes and EF. In a study of normal volunteers and hypertensive patients CMR was found to be more reliable and precise in measuring LV mass compared to transthoracic echocardiography. (5) Multiple studies have demonstrated the accuracy and reproducibility of CMR for measuring LV volumes and EF, including comparisons to LV angiography (6), gated single photon emission computed tomography (7) and echocardiography. A study by Bellenger el al compared CMR to echocardiography for ventricular analysis in patients with heart failure and normal volunteers.(8) Using CMR the sample sizes needed to detect 10-ml changes in end-diastolic (n=12) or end-systolic volume (n=10) or a change in EF of 3% (n=15) are much lower than with echocardiography. As a result, CMR analysis of LV volumes and EF has the potential to save time and reduce cost in studies of heart failure patients. Nowosielski et al compared CMR to echocardiography in patients treated for first acute MI with primary angioplasty and found no significant difference in estimation of EF, with the exception of patients with posterior infarctions. (9) The authors asserted that biplane echocardiography may fail to detect wall motion abnormalities in areas difficult to visualize with a transthoracic ultrasound, such as the posterior wall.

In a recent study by Bodi et al, 214 patients with a first ST elevation MI were treated with thrombolytics or angioplasty and studied with a comprehensive CMR exam within 7 days of their infarction. (10) The CMR study included wall motion analysis at rest and after low-dose dobutamine as well as characterizing the presence of MO and transmural infarction. The degree of systolic dysfunction and extent of transmural necrosis provided independent prognostic information.

1.b Late Gadolinium Enhancement

1.b.1 Initial Validation of Late Gadolinium Enhancement—The duration of myocardial ischemia is directly related to the extent of tissue necrosis and infarct size. Tissue ischemia begins in the subendocardium since it has the highest metabolic demands. With prolonged ischemia, the degree of infarction can extend from the LV subendocardium to involve the entire wall. In the setting of MI, administration of intravenous gadolinium will result in delayed myocardial enhancement due to disrupted myocyte membranes which allow extracellular gadolinium to freely diffuse into previously intracellular space. (11) With chronic infarction, the damaged myocytes are replaced by collagenous scar with relatively increased interstitial volume allowing for an increased concentration of gadolinium in the scar.

The use of late gadolinium enhancement to evaluate areas of myocardial scar has been extensively validated in both animal and clinical studies since the 1980's. One of the earliest animal studies demonstrated time variable changes in T1 and T2 relaxation times in canine myocardium after administration of gadolinium compared to dogs that did not receive gadolinium. (12) Dogs with surgical ligation of the LAD that received gadolinium had greater T1 shortening seen with infarcted areas compared to normal myocardium. The dominant effect of gadolinium-chelates on myocardium is shortening of T1 which results in increased signal intensity in areas of scar compared to normal myocardium.

To evaluate the effect of establishing reperfusion with acute MI, Judd et al performed the first study of CMR imaging of a canine model of acute, reperfused anterior MI 48 hours after the infarct.(13) CMR imaging occurred 48 hours after reperfusion and was immediately followed by fluorescent dye thioflavin-S, which was injected into the left ventricle to define the region of no-reflow and the canine hearts were analyzed ex-vivo with triphenyltetrazolium choride (TTC), ultraviolet light for thioflavin and microsphere counting for regional blood flow. Area at risk was defined as reduction in myocardial blood flow by at least 50% based on the microspheres. After gadolinium based contrast administration,

three distinct patterns were identified: 1) normal remote myocardium had a diffuse increase in signal intensity over the first minute which subsequently decreased, 2) central subendocardial hypoenhancement in the infarct region which was most apparent within the first two minutes and had a slow increase in signal intensity, and 3) areas of hyperenhancement which became delineated from normal myocardium after 5 minutes and persisted for the 15 minutes of imaging. The area of hyperenhancement (8.4±2.2%) was approximately half the size of the region at risk (23.5±2.9%) and the areas of hypoenhancement had a high degree of correlation with the area of no-reflow outlined by thioflavin. There was a strong correlation between the amount of hyperenhancement and the infarct size measured by the TTC negative area on histology.

Kim et al carefully validated late enhancement imaging with the extent of myocardial necrosis seen in histologic sections treated with TTC in a canine myocardial model of infarction, finding excellent correlation (Figure 1). (14) This landmark study of infarct size assessed by myocardial histology compared to CMR images demonstrated consistent correlation at day 3 after infarction. The question of whether ischemic but non-infarcted myocardium exhibited the same properties of enhancement with gadolinium was answered by Fieno et al who used fluorescent beads to define ischemic but viable myocardium which did not enhance after gadolinium infusion. (15)

In a human study of acute infarction, serial CMR images were obtained after giving gadolinium to evaluate for time dependent changes in normal and infarcted myocardium. (16) The ratio of increased signal intensity for infarcts versus normal myocardium reached a maximum at 15-20 minutes after administration of gadolinium and was not significantly different at 25-30 minutes. In addition, these authors found similar intensity of late gadolinium enhancement (LGE) in reperfused and non-reperfused infarction as well as describing varying patterns of LGE including subendocardial and transmural. Lima et al. studied patients after acute MI with CMR, X-ray angiography and thallium scintigraphy to determine if CMR provides additional information about myocardial damage after acute MI. (17) Short axis images acquired 160 seconds after contrast demonstrated central hypoenhancement in the infarcted region. Subsequent images obtained after 10 minutes revealed hyperenhancement of the infarcted region surrounding the initial area of central hypoenhancement. The subendocardial hypoenhancement was related to reduced TIMI flow (0 or 1) in the infarct-related artery. The summed area of late enhanced and central hypoenhanced myocardium on CMR images were compared with the fixed single photon computed tomography (SPECT) thallium defects on the same images and demonstrated good correlation ($r=0.92$, $p<0.001$).

1.b.2 Imaging Sequences for LGE—The optimal methodology, an inversion recovery pulse sequence, for imaging late gadolinium enhancement was described by Simonetti and colleagues in 2001. (18) There are now multiple approaches to using this pulse sequence to image late gadolinium enhancement which all take advantage having the inversion time set to null normal myocardium. Against the dark background of normal myocardium, LGE appears as white or light grey (Figure 2).

Early LGE imaging techniques used spin echo sequences however these were limited by significant respiratory motion artifact. Current techniques allow for high resolution CMR images to visualize large transmural infarcts as well as small subendocardial infarcts due to high spatial resolution of 1x1x3mm and temporal resolution of 15-50ms. (19) The technique for imaging LGE uses electrocardiographic (ECG) gating with data acquired every other heart beat for adequate relaxation between inversion pulses. A breath-held inversion-recovery segment gradient-echo sequence produces strongly T1 weighted images due to the inversion pulse before imaging and acquires a single image over several cardiac cycles. (18)

With the inversion recovery pulse sequence using magnitude-reconstructed images, the signal intensity between normal and infarcted segments increases by 500-1000%. (20) The traditional gradient-echo inversion recovery imaging requires setting a specific inversion time for each patient where the myocardium is nulled. However, with the advent of phase-sensitive inversion recovery sequences, the phase-sensitive detection can remove the background phase while preserving the correct magnetization during the inversion recovery. (21) The background phase includes off-resonance effects and contributions to variation in signal intensity from surface coils and receivers. When comparing phase-sensitive and magnitude images, a benefit of phase-sensitive imaging is maintaining excellent image contrast over a range of inversion times. There is a similar infarct size when using either the phase-sensitive or magnitude images.

Traditionally images are obtained during a breath-hold. However newer techniques incorporate faster imaging sequences to allow for subsecond free-breathing acquisition of LGE images. (22) The sensitivity of the single-shot inversion recovery, steady state free precession LGE imaging was moderately reduced (87%) compared to a standard technique of segmented inversion-recovery gradient-echo (98%); however, the specificity was excellent (96%). The reduction in sensitivity for detection of MI with single-shot LGE imaging was largely in the setting of small or subendocardial infarcts, likely due to the reduced spatial resolution and differences in tissue contrast with this technique. Given the reduction in sensitivity and tendency to underestimate the size of infarction and extent of transmural infarction with the single-shot imaging, it is considered the preferred approach only in patients who are unable to hold their breath adequately.

1.b.3 Quantifying LGE and Reproducibility—The infarct size can be measured using planimetry of myocardial segments with LGE seen on sequential short axis images of the left ventricle. The degree of infarct transmurality is measured by dividing the area of hyperenhancement by the thickness of the myocardium in that segment (Figure 3). In order to establish a uniform means of quantifying the degree of LGE, visual analysis of areas of LGE were analyzed by experienced observers after adjusting the threshold setting of the images at 2, 3, 4, 5 and 6 standard deviations (SD) above the mean signal intensity of normal remote myocardium in the same image slice. (23) The total infarct size was significantly affected by the stepwise increase in windowing threshold with an increase in size of 40% for 2 SD, 31% for 3 SD, 17% for 4 SD and a non-significant 7% decrease for 6 SD. The location of myocardial LGE is visually assessed using the AHA 17-segment model (2) and the infarct size is characterized by degree of transmurality (0-25%, 26-50%, 51-75% and greater than 76%). (24) The degree of LGE can also be measured as a percentage of LV mass by identifying the sum of hyperenhanced pixels on each LV short axis image, divided by the total number of LV myocardial pixels. (25)

The severity of myocardial necrosis resulting from acute MI can be gauged by the degree of elevation in cardiac enzymes such as CK-MB or troponin. Choi et al found a strong correlation between infarct size on LGE with CMR and peak CK-MB values ($r=0.90$, $p<0.001$) with a corresponding relationship of peak CK-MB value and infarct mass ($r=0.83$, $p<0.01$). (26) Furthermore, Choi found that greater than 75% transmurality of an acute infarct indicated a 5% chance of functional recovery, compared to myocardial segments without LGE which had 80% likelihood of recovering normal function. (26)

Ortiz-Perez et al investigated the relationship between the 17 segment AHA model to characterize LGE patterns with the culprit vessel on X-ray angiogram in over 90 patients after acute MI (27). The authors found presence of LGE in the basal anteroseptum, mid anterior or anterseptal or apical anterior walls has 100% specificity for left anterior descending artery occlusion. In contrast, no segments were 100% specific for either right

coronary artery or left circumflex artery occlusion. Furthermore, the number of myocardial segments demonstrating LGE in the setting of LAD infarcts is larger than the AHA 17-segment model.

A recent large multi-center trial evaluated the performance LGE imaging using gadolinium to detect the presence of MI. (28) Over 280 patients presenting with initial diagnosis of MI were enrolled in both an acute and chronic MI arm. Patients were randomized to receive one of four doses of gadoversetamide (0.05, 0.10, 0.20 or 0.30 mmol/kg). The LGE images were obtained beginning at 10 and 30 minutes after the administration of contrast. There was no difference in diagnostic performance at 0.20 mmol/kg when obtaining LGE images after a delay of 10 or 30 minutes. The accuracy of LGE for identifying the correct infarct location based on angiography was 91% for the 0.20 mmol/kg dose compared to 95% for the 0.30 mmol/kg dose. The accuracy of the 0.10 mmol/kg dose was only 79% which indicates a diagnostic advantage when using contrast doses at 0.20 mmol/kg and above for this particular gadolinium chelate.

In order to test the reproducibility of LGE imaging in patients with acute MI, Wagner et al evaluated the effect of timing and dose of gadolinium as well as varying inversion times at a multi-center study. (29) An important finding was that measurement of infarct size with LGE is independent of the timing and dose of gadolinium as long as the inversion time is adjusted appropriately and the LGE images are acquired within the framework of 5-30 minutes after giving a contrast dose of 0.1-0.2 mmol/kg.

1.b.4 Comparison of LGE to SPECT Imaging in Patients—Before the use of CMR imaging with LGE to identify areas of MI, there was a robust amount of literature using nuclear imaging with SPECT for evaluation of ischemia and infarction. SPECT cameras have lower resolution that CMR and image quality can also be challenged by respiratory motion or signal attenuation from nearby breast or intestine. In the setting of patients with known or suspected coronary artery disease (CAD), Wagner et al found that all myocardial segments with near transmural infarction on LGE were also detected with SPECT. (30) However, 47% of the myocardial segments with evidence of subendocardial infarction on LGE were missed by SPECT imaging (Figure 4). The increased sensitivity of CMR with LGE imaging to detect subendocardial infarction was attributed the approximately 60-fold greater spatial resolution than SPECT. In the same paper, Wagner et al used histochemical staining of infarcted canine hearts as the gold standard for comparison with LGE and SPECT. Both techniques correctly identified all infarctions involving greater than 75% of the myocardial wall. However, segments with subendocardial infarctions were seen in 92% of LGE images and only 31% of SPECT studies

CMR and SPECT imaging have also been compared in the setting of acute MI treated with revascularization. Ibrahim et al imaged almost 80 patients one week after acute MI and found CMR with LGE was superior to SPECT in detecting acute MI (overall sensitivity: 97% vs. 87%; p =0.008). (31) In particular, CMR with LGE was more sensitive for detection of small infarctions as measured by peak troponin T level less than 3.0 ng/ml (92 vs. 69%; p =0.03) and non Q-wave infarctions (sensitivity 85% vs. 46%; p=0.06). In addition, differentiation of the infarct-related artery with CMR using LGE was superior to SPECT imaging.

1c. Infarct Size, Infarct Detection, and Prognosis

Measuring the size of myocardial infarction in the acute versus the chronic setting will result in different estimations of degree of infarction. In the acute phase of infarction, the volume of myocardium affected can be up to 25% greater due to tissue edema, hemorrhage and inflammation. (32) Animal studies revealed the first insight that infarct mass decreases over

time and does so more rapidly in the setting of reperfusion. (33) In a study of more than 30 patients with an acute MI, the peak troponin and degree of wall thickening were related to the size of acute infarction measured with LGE. (34) The study patients had follow-up CMR imaging 2 months after the acute infarction. The chronic infarct size was reproducible but was significantly smaller (11±9%) than measured during the acute infarct phase (16±12%), $p<0.003$. Choi et al revealed further insight into the process of infarct involution over time by studying 25 patients with CMR at one and eight weeks after reperfused infarction. (35) Over the 8 weeks of infarct healing, there was a 26% decrease in the total infarct size (LGE and MO along with an 11% decrease in infarct transmurality. Interestingly, infarcts with greater degree of MO showed a trend towards a greater degree of infarct involution, potentially related to the more severe initial ischemic insult.

In the setting of an acute MI, the transmurality of LGE imaging has important prognostic significance. In the study by Bodi et al, there was a significant difference in major adverse cardiac events (MACE) rate when comparing patients with 5 or more segments of transmural infarction compared to those with less involved myocardium, (23% versus 5%, $p<0.001$). (10) In addition to cardiovascular events, the transmural extent of LGE in the setting of reperfused acute MI also predicts long term improvement in that area of dysfunctional myocardium when patients were re-imaged with CMR 2-4 months after infarction. (26) The infarct size measured by LGE predicts LV remodeling with an area under the ROC curve of 0.891 (36) In addition, the risk for LV remodeling increased 2.8 fold with each 10% increase in size of infarct seen on LGE. There was also an association between remodeling and larger infarct remodeling seen on follow-up imaging at 8±3 months after initial reperfused infarction.

In a study of 122 patients with percutaneous revascularization after ST-elevation MI, the acute infarct size with LGE correlated with EF and LV volumes indexed for patient body surface area as well as patient outcomes of death, recurrent MI or heart failure. (37) However, on multivariable analysis, infarct size was the only significant predictor of adverse events. When the patients were followed with repeat CMR at 4 months, all patients had improved EF and those in the largest infarct tertile had an improved EF (32%±9%) to (36% ±11%), $p = 0.002$) at the expense of a significant increase in end-diastolic volume 86±19 to 95±21 ml/m^2, $p = 0.005$. The key finding from this study was that acute infarct size directly relates to LV remodeling and is a stronger predictor of clinical events than systolic function.

One of the first studies to link the time of coronary vessel occlusion and degree of MO and transmural necrosis was published in 2005 by Tarantini et al. (38) Patients with reperfused ST-elevation MI were stratified based on achieving adequate epicardial vessel flow during the catheterization with TIMI grade flow of 3 or not. Despite similar delay in reperfusion for the group with TIMI grade 3 flow and those with TIMI grade flow < 3, there was a higher percentage of patients with transmural necrosis and MO in the latter group. In patients with TIMI grade flow < 3, there was a continuum of myocardial necrosis and MO seen on CMR imaging with each 30-minute delay in successful percutaneous coronary intervention associated with an increased risk of transmural necrosis by 37% and MO by 12%. In all patients, regardless of TIMI grade flow, the probability of transmural necrosis was higher than that of MO suggesting that the pathophysiology underlying MO may occur later than transmural infarction. The study lends credence to the importance of quickly restoring epicardial coronary artery flow with the goal of reducing the degree of transmural necrosis and microvascular dysfunction.

Patients with suspected CAD but absence of electrocardiographic Q-waves were studied by Kim et al using LGE to identify the prevalence and prognosis of unrecognized MI. (39) The prevalence of unrecognized non-Q-wave MI in patients at risk of CAD was 27%, based on

findings of LGE in a coronary distribution. The patients with a new diagnosis of CAD based on the LGE were more likely to be older, have a higher Framingham risk score and have diabetes. This important study underscores the high frequency of undiagnosed MI in patients at risk for CAD and furthermore the presence of unrecognized MI was an independent predictor of all-cause mortality (hazard ratio 11.4, 95% confidence interval: 2.5–51.1) and cardiac mortality (hazard ratio 17.4, 95% confidence interval: 2.2–137.4).

In a large study, 195 patients without known MI were evaluated for presence of LGE indicating a previously unrecognized MI. The patients were referred for clinical CMR given concern for CAD based on symptoms or a viability evaluation in the setting of angiographic CAD. (40) There were 170 patients without Q waves on EKG and 37 of these patients (22%) had evidence of LGE with a resulting significant association with major adverse cardiac events (HR, 7.39; $p<0.0001$) and cardiac mortality (HR, 8.15; $p=0.0003$). By multivariable analyses, LGE was independently associated with MACE above and beyond the clinical model alone ($p<0.0001$) or combined with significant stenosis on angiogram ($p=0.0007$), LV EF ($p=0.001$), LV end-systolic volume index ($p=0.0006$), or segmental wall motion abnormalities ($p=0.002$). In fact, LGE was the strongest predictor in the overall model for MACE and cardiac mortality. In addition, there seemed to be a “threshold-effect” wherein patients with smallest percentage of LGE (mean, 1.4±1.1%) had a greater than 7-fold hazard increase for MACE ($p=0.0002$) compared to those without LGE. This important study highlights the incremental prognostic value of LGE even in the setting of a small degree of involved myocardium.

A study which validated the high prevalence and associated risk of clinically unrecognized MI in diabetic patients without a known history of CAD was performed by Kwong et al. (41) The study involved over 180 diabetic patients divided on the presence of Q waves on their baseline electrocardiograms. The main finding was that LGE consistent with myocardial scar from unrecognized MI occurred in 28% of patients. In this group of patients with diabetes and no evidence of MI on electrocardiogram, the presence of LGE was the strongest multivariate predictor of death and major adverse cardiovascular events. LGE provides for an assessment of prior unrecognized MI in the setting of a normal EKG as well as normal LV wall motion and function. Identifying patients at increased risk for death and adverse events from undiagnosed MI provides an opportunity to proactively modify their risk of future events.

A comprehensive CMR exam including contrast-enhanced myocardial perfusion imaging with LGE imaging was performed in 254 patients with symptoms of myocardial ischemia. (42) After adjusting for patient age and gender, reversible perfusion defects and LGE had complementary prognostic value with both associated with greater than 3-fold increase risk of death or MI. For patients with normal stress myocardial perfusion and no prior history of MI, the presence of LGE was associated with greater than 11-fold hazards increase in death or MI. If patients had a CMR exam without perfusion defect or LGE, they had an excellent event-free prognosis with a 98.1% negative annual event rate for death or MI.

1.d Peri-infarct (“gray-zone”) Enhancement

The concept of peri-infarct zone enhancement was promoted by Schmidt et al wherein tissue heterogeneity at the borders of infarcted myocardium can be imaged with contrast-enhanced CMR and is related to increased susceptibility to ventricular arrhythmia. (43) The study investigated patients with ischemic cardiomyopathies referred for implantable cardiac defibrillators in order to determine if heterogeneity in peri-infarct regions can be established using contrast-enhanced CMR with the idea that adjacent areas of necrosis and viable myocardium could be fertile ground for re-entrant arrhythmias. (44) To quantify the peri-infarct zone, Schmidt et al first traced the endocardial and epicardial borders in sequential

short axis images and the region of high signal intensity was outlined and maximum intensity generated. The infarct core was defined as myocardium with signal intensity greater than 50% maximum. Tissue heterogeneity in the infarct periphery or "gray zone" was defined as having signal intensity greater than that of remote myocardium but less than 50% of the maximum.(Figure 5) The region of intermediate late gadolinium enhancement, characterized as the "gray zone" at the periphery of myocardial scar is related to inducibility of monomorphic ventricular tachycardia. Criticism of the "gray zone" theory centers on concern for partial volume effects at the border of normal and infarcted myocardium. In addition, there is as of yet no standardization between laboratories of methodologies used to measure the area of gray zone.

Yan et al tested the hypothesis that the degree of gray-zone measured by contrast-enhanced CMR would be an independent predictor of mortality post-MI. (45) In this study, the total infarct size was measured semi-quantitatively and divided into the core region (greater than 3 SD above normal remote myocardium) and the gray zone or peri-infarct regions (with signal intensity between 2-3 SD above normal myocardium). Then, the peri-infarct zone was normalized as a percentage of the total infarct size. After adjusting for age and LV EF, the normalized peri-infarct zone was independently associated with all-cause and cardiovascular mortality (adjusted HR, 1.42 and 1.49, respectively). This study sheds light onto a potential mechanism for increased mortality in patients post-MI.

Patients with ischemic cardiomyopathy referred for ICD were evaluated by contrast-enhanced CMR to establish a relationship between extent of peri-infarct gray-zone and spontaneous ventricular arrhythmia. (46) Roes et al found the presence of peri-infarct tissue heterogeneity on contrast-enhanced MRI in patients with prior MI to be a stronger predictor of spontaneous ventricular arrhythmia and ICD therapy when compared to total infarct size and LV function. Ultimately, a correlation between the extent of gray-zone and post-MI arrhythmia may lead to a refinement in which patients with ischemic cardiomyopathy will derive the most benefit from an ICD.

Patients with co-existing renal failure, glomerular filtration rate of 30 ml/min/1.73m^2 should not receive gadolinium due to the potential risk of developing nephrogenic systemic fibrosis. (47) As a result, patients with severe renal failure cannot undergo contrast-enhanced CMR imaging to assess for myocardial scar.

1.e Microvascular Obstruction

MO occurs when a patient with acute MI achieves epicardial coronary artery reperfusion, however not complete myocardial reperfusion – this has also been called "no-reflow." (48) The consequences of MO are significant, with patients suffering higher rates of post-infarction complication, mortality and adverse LV remodeling. Niccoli et al asserts that the pathology underlying MO involves distal embolization and ischemic-reperfusion injury in the setting of susceptible coronary microvasculature. (48) The resultant myocardial necrosis from ischemia results in an inflammatory cascade which damages the microcirculation with neutrophil accumulation, endothelial swelling and capillary compression by surrounding edematous myocytes. (49)

The presence of MO with CMR is identified by the lack of subendocardial contrast uptake in an area surrounded by enhancement on LGE imaging or early hypoenhancement seen in the first few minutes after first-pass contrast-enhanced perfusion imaging, so-called early enhancement imaging (Figure 6). (17)

Rogers et al studied patients on day 4 and 7 weeks after acute MI and found that regions of MO were predictive of non-viable myocardium since there was no recovery of segmental

LV contractile function in the regions of MO. (50) Nijveldt et al explored the relationship between angiographic, electrocardiographic and CMR assessment of MO after reperfusion for acute MI. (51) Evidence of early MO on first pass perfusion was identified by a qualitative region of hypoperfusion in the subendocardium that persists for more than one minute. On the LGE images, late MO was defined as any region of hypoenhancement surrounded by an area of hyperenhancement seen 12-15 minutes after contrast administration. Early MO was seen in 68% of patients whereas only 57% had late MO. Other studies have also found a lower prevalence of late MO, likely due to the slow contrast diffusion into myocardium with less severe MO resulting in smaller regions of hypoenhancement on the LGE images. (52) However, the presence of late MO on baseline study was the strongest predictor of change in LV EF and end-systolic function after 4 months. (51)

The presence of MO helps in determining the acuity of the MI as it only occurs in acute infarcts and persists for at least 9 days. (53) MO is not typically seen in chronic infarction. Wu et al used a canine model to correlate MO measured with microspheres, contrast-enhanced echocardiography and CMR imaging with good correlation with histopathology. (53) The authors also found the extent of MO measured with contrast-enhanced CMR was unchanged at 2 and 2 days after MI and MO was completely resolved by the follow-up imaging at 6 months.

Kwong et al studied the role of resting first-pass perfusion imaging and LGE to identify acute coronary syndrome in patients presenting with chest pain. (54) Acute coronary syndromes were diagnosed with a sensitivity of 84% and specificity of 85% based on LGE or the presence of a resting perfusion abnormality indicative of MO.

It is well established that the presence of MO predicts poor functional recovery in the infarcted myocardium. (55) The presence of MO after a reperfused MI is associated with increased cardiovascular events (Figure 2) as shown by Wu et al in 44 patients with MO indicated by areas of hypoenhancement 1-2 minutes after administration of contrast. (56) The absence of MO predicted event-free survival compared to patients with MO over the study period of 25 months. In addition, the presence of MO was significantly associated with LV remodeling and post-infarction complications.

A large study by Hombach et al of 110 patients with acute MI demonstrated that MO is more important than EF when predicting post-MI LV remodeling and survival. (57) In the setting of reperfused MI, the EF improves despite the size of infarcted myocardium due to the recovery of stunned myocardium in the infarct zone. (58) However, patients with acute MI and evidence of MO on LGE images, when imaged 8 weeks after infarction, have no improvement in their EF compared to those without the presence of MO. (59)

1.f Area at Risk

Myocardial edema occurs in the setting of acute MI due to disruptions in myocellular membrane integrity (Figure 7) and worsens in the setting of reperfusion. (60) Advances in CMR technology now allow for high resolution black blood images using T2-weighted signal. The T2 signal intensity appears to be related to myocardial water content, however studies have shown variable amounts of water content in acute infarctions, ranging from 3% to 28%. (61). In an animal model of transient coronary occlusion and reperfusion, Aletras et al found good correlation in terms of size and location between areas of hyperintensity on T2-weighted images and area at risk (AAR) seen by microspheres in a transient coronary occlusion/reperfusion model. (62) The AAR based on T2-weighted images was larger than the area of infarction seen with LGE and demonstrated partial functional recovery over a two month period. The authors also used a clinical model of patients presenting with a ST-

elevation MI and reperfusion which demonstrated identification of myocardial AAR with increased T2 weighted signal on CMR imaging.

Abdel-Aty et al also found that myocardial edema seen with increased signal intensity on T2 weighted imaging occurs in acute ischemic injury and is a marker of reversible injury. (63) Patients with a first MI were studied with CMR imaging using T2-weighted triple inversion recovery sequence and contrast-enhanced inversion recovery gradient echo sequence at two time points: one day post-infarction and then 3 months later. In the acute setting, all myocardial segments with higher signal-to-noise ratio than surrounding normal myocardium matched the region supplied by the infarct related artery. When patients with acute versus chronic MI were compared, those with chronic infarction demonstrated no difference in the signal-to-noise ratio between infarcted and remote myocardium on T2-weighted imaging.

Friedrich et al. retrospectively evaluated patients with acute MI and found the AAR determined by increased T2-signal within several days of reperfusion was transmural and larger by 16±11% than the area of irreversible injury determined by LGE. (64) The ability to accurately identify AAR using T2-weighted CMR will be helpful as a clinical trial endpoint for studying myocardial salvage with reperfusion therapies.

A recent paper by Arheden et al was the first study to validate T2-weighted imaging with SPECT in patients after MI. Sixteen patients with first ST-elevation MI received a radio-labeled nuclear tracer prior to undergoing percutaneous coronary intervention with subsequent SPECT imaging within 4 hours. (65) CMR studies with T2-weighted imaging occurred at one day, one week, 6 weeks and 6 months after infarct, but gadolinium was given only at one week for quantification of infarct size. At one day, the AAR on SPECT was 33±10% of the LV myocardium and was not significantly different from that measured with T2-weighted images, 29±7%. Over time, the AAR as measured by SPECT and T2-weighted images decreased. Advantages of CMR versus SPECT for characterizing AAR include the lack of radiation and higher spatial resolution, allowing for a complete myocardial evaluation post-infarction and the fact that only one imaging session is needed. The authors defined salvaged myocardium as AAR minus the final infarct size and promoted the use of CMR to characterize myocardial salvage in the setting of acute MI without needing to interfere with patient care during the initial treatment for the MI.

Mikami et al investigated whether detection of myocardial edema with T2-weighted CMR imaging is influenced by the presence of MO in patients with acute MI (Figure 8). (66) They found a significantly lower SI on T2-weighted images in areas of MO compared to areas of LGE without MO; however, infarct-associated edema in areas without MO could be easily detected using T2-weighted imaging.

The addition of T2-weighted imaging to a CMR protocol used for emergency department patients presenting with chest pain, negative biomarkers and no ischemic ECG changes increased the overall accuracy for detecting acute coronary syndromes from 84% to 93% and added significant value to traditional risk factors and clinical assessment. (67)

There are exciting advances being made in the field of characterizing AAR with CMR studies using T2-weighted images. However there exist several limitations which reduce current clinical applicability. Image quality with T2-weighted CMR sequences can be limited and preclude automated segmentation of the involved myocardium. (65) In addition, pulse sequences for T2-weighted imaging such as T2-weighted fast spin echo can have a lower signal-to-noise ratio which can influence the sensitivity of the imaging. A theoretical difficulty with T2-weighted imaging is areas of slow blood flow in the LV cavity apex can have increased signal intensity and appear as areas of myocardial edema. However, newer pulse sequences for T2-weighted imaging are being evaluated to address these issues. (68)

1.g. First-pass Contrast Enhanced CMR

Myocardial perfusion with CMR uses contrast-enhanced first pass imaging to take advantage of the T1 shortening effect of gadolinium contrast. The degree of increase in contrast signal intensity is determined by the concentration of gadolinium, degree of blood flow as well as the type of pulse sequence used. Gadolinium causes an increase in signal intensity on T1-weighted images resulting in a gray appearance of well-perfused myocardium. The CMR imaging protocol for first pass-perfusion involves magnetization preparation with saturation recovery and pulse sequences of either gradient recalled echo (GRE), hybrid GRE with echo-planar imaging (GRE-EPI) and balanced steady-state free precession (SSFP). (69) The key differences in choosing a pulse sequence for first pass perfusion involve SSFP with the highest contrast-to-noise ratio but a longer acquisition time leading to motion artifact and GRE-EPI having the largest spatial coverage and shortest imaging time, however a lower contrast-to-noise ratio.

For optimal first-pass perfusion imaging, several pre-requisites are necessary: adequate temporal resolution to image several short axis slices each heartbeat in order to visualize the initial contrast bolus, high spatial resolution to distinguish between subendocardial and subepicardial myocardium, adequate number of short axis slices to have representative coverage of the myocardium, linear relationship between contrast dose and corresponding signal intensity and a significant difference in post-contrast appearance of normal and ischemic myocardium. (70)

In patients presenting with acute coronary syndrome with coronary lesions of unclear significance on cardiac catheterization, first pass-perfusion with stress and rest imaging can identify the anatomic region with impaired perfusion and therefore guide the intervention. First pass perfusion imaging uses a low dose (0.05-0.1 mmol/kg) of gadolinium with 3-5 short axis images with a slice thickness of 8mm which are acquired as the contrast is infused. The imaging occurs every heart beat for 40-50 beats in order to allow all of the contrast to pass through the left ventricle myocardium. (24) With stress CMR, the study begins with the use of a vasodilator (adenosine, regadenoson or dipyridamole) followed by first pass perfusion to acquire the “stress” images. The vasodilators affect adenosine subtype 2 receptors in the coronary vasculature, causing hyperemic vasodilation unless there is a significant coronary atherosclerosis in which cases there is relatively less vasodilation and resultant distal flow. Areas of ischemia have reduced signal intensity compared to normal myocardium on T1-weighted images allowing for differentiation as a perfusion defect on stress imaging. (71) After 10 minutes, the resting perfusion images are obtained. A perfusion defect seen on stress imaging but absent at rest indicates reversible ischemia (Figure 9). However, a perfusion defect seen on both stress and rest imaging is consistent with prior infarction. Acquisition of the LGE images follow after 5 minutes using inversion recovery gradient pulse sequences. LV functional images in the long axis (2, 3 and 4 chamber) as well as series of 8-10 short axis images covering the left ventricle can be acquired in the period between the stress and rest perfusion sequences. The presence of scar or MO on LGE aids in differentiating prior MI from a dark rim artifact seen with perfusion imaging. If there is a perfusion defect apparent at both rest and stress images, but no evidence of LGE, then the perfusion abnormality does not indicate prior infarction, but rather artifact.

In a multi-center trial of 212 patients with known CAD evaluated with adenosine perfusion-CMR and SPECT to identify lesions with greater than 50% diameter stenosis on angiography, adenosine perfusion-CMR had better diagnostic performance based on the area under the ROC curve (0.86±0.06 versus 0.75±0.09, p=0.013). (72) Nandular et al studied the test characteristics of stress CMR studies with perfusion imaging to diagnose CAD based on patients with known X-ray angiography demonstrating a greater than 50% diameter stenosis as the reference standard. (73) Perfusion-CMR had a sensitivity of 0.91 and specificity of

0.81 for the diagnosis of CAD lesions with a greater than 50% stenosis on the patient level. Klem et al. found an additional benefit for the diagnostic accuracy of stress CMR by including data from LGE images into the analysis algorithm, giving a sensitivity of 89% and specificity of 87% for the diagnosis of CAD with coronary stenosis greater than 70% or left main disease greater than 50%. (74)

In the setting of acute coronary syndromes, Plein et al found a comprehensive CMR exam including perfusion defects, segmental wall motion abnormalities, LGE and coronary analysis had a sensitivity of 96% and a specificity of 83% for the detection of significant CAD. (75) In this study, patients with acute coronary syndromes who had low-intermediate risk TIMI scores, the comprehensive CMR exam was more sensitive than the TIMI risk score in identifying significant CAD.

The current clinical practice is to perform myocardial perfusion imaging with CMR using scanners with a magnetic field strength of 1.5-Tesla (T). Using 3-T systems allows for increased signal-to-noise ratio and contrast enhancement. (76) Given the improved spatial resolution at 3-T, Cheng et al found perfusion imaging at 3-T to have a higher diagnostic performance in identifying single vessel and multivessel disease compared to 1.5T, however there was no difference in the overall detection of coronary disease in their cohort of patients referred for diagnostic angiography to evaluate chest pain. (77)

1.h Evaluation of Left Ventricular Thrombus

An additional benefit of performing post-contrast imaging in patients after acute MI, particularly those with depressed systolic function, is identification of LV thrombus which is seen as an area of absent contrast uptake on post-contrast cine or LGE images. (78) In a large study of 361 patients with ischemic heart disease, Srichai et al. found a combination of LGE and post-contrast cine imaging had a sensitivity of 88% and specificity of 99% for LV thrombus. (79) The study used either surgical or pathologic confirmation of the thrombus. CMR with LGE and post-contrast cine imaging had superior sensitivity to echocardiography (either transthoracic or transesophageal) for the detection of LV thrombus. Weinsaft et al studied 784 consecutive patients with systolic dysfunction (EF less than 50%) for prevalence of LV thrombus identified by absent contrast uptake on LGE. (80) In this population, 7% of patients had LV thrombus found by LGE imaging and the use of cine SSFP imaging was less sensitive than LGE for detection of thrombus, particularly with small intra-cavitary or mural thrombus.

1.i Evidence of Myocardial Necrosis without Significant Underlying CAD

Patients presenting with chest pain and positive biomarkers but with no significant CAD at cardiac catheterization are excellent candidates for CMR to evaluate the etiology of their chest pain by looking for evidence of patterns of LGE. Assomul et al evaluated 60 patients with troponin-positive chest pain and non-obstructive CAD on X-ray angiography and identified a reason for the clinical presentation in 65% of patients. (81) The most common cause of chest pain and positive troponin in this cohort was myocarditis (50%), MI (11.6%) and non-ischemic cardiomyopathy (3.4%).

2. Assessment of Myocardial Viability prior to Revascularization

The assessment of myocardial viability plays an important role when choosing patients for revascularization who have impaired LV function or who have epicardial coronary artery stenosis of undetermined significance. Dysfunctional myocardium that has contractile reserve with the potential for recovery of LV function after revascularization is considered viable. (82) Patients with CAD may have dysfunction but viable myocardium in two different settings, those with an acute MI may have stunned myocardium and those with

chronic ischemia have hibernating myocytes. Contrast-enhanced CMR using gadolinium generates a complete assessment of myocardial viability based on LV functional analysis, perfusion abnormalities and the presence of scar with LGE (Figure 10).

Identifying patients likely to benefit from revascularization in the setting of chronic LV dysfunction with viable myocardium will result in lower mortality for those revascularized during the peri-procedure period as well as a long term mortality benefit. (83) Establishing patients with adequate viable myocardium prior to revascularization has significant prognostic importance. A meta-analysis from 2003 evaluated more than 3,000 patients with ischemic cardiomyopathy and average EF of 32% who were revascularized. (84) In patients with viable or hibernating myocardium, as determined by SPECT myocardial perfusion imaging PET or dobutamine echocardiography, there was lower mortality (3.2% versus 16%, $p<0.0001$) than those treated medically for chronic CAD.

LV wall thickness on rest cine CMR imaging of less than 5.5mm at end-diastole is one marker of non-viable myocardium (85). However non-transmural infarcts typically don't result in severe LV end-diastolic thinning. In patients with transmural infarcts, the process of infarct healing and subsequent myocardial wall thinning can take up to 4 months. (86) Segmental LV wall thickening is quantified by using a software analysis package to draw contours around the endocardial and epicardial borders. The systolic segmental wall thickening can then be calculated by subtracting the end-diastolic wall thickness from the end-systolic measurement. Segmental wall thickening measured with CMR less than 30% is correlated with reduced EF. (87) Schinkel et al pooled the analysis of 3 CMR studies which used end-diastolic wall thickening to predict viability with good sensitivity (95%) and negative predictive value (92%). However this is limited by poor specificity (41%) and positive predictive value (56%). (88)

SSFP cine imaging of the left ventricle in the 2, 3 and 4 chamber long axis, as well as a stack of short axis images throughout the ventricle, performed at rest and after administration of low dose dobutamine (10 μg/kg/min) can assess contractile reserve and predict areas of functional recovery with revascularization. (89) Low-dose dobutamine has also been used to evaluate myocardial viability with magnetic resonance tissue tagging to quantify regional intramyocardial function. (90) Myocardial tagging uses radiofrequency and gradient pulses to place a grid of nulled orthogonal lines made up of saturated rows of protons over the heart at end diastole. (91) The tags deform during the cardiac cycle and regional dysfunction can be assessed qualitatively as lack of tag deformation and quantitatively with one, two, or three-dimensional analytic approaches.

Evaluating myocardial viability in the setting of ischemic cardiomyopathy is well established using nuclear imaging. Kuhl et al compared SPECT, 18F-fluorodeoxyglucose (FDG) positron emission tomography (PET) and contrast-enhanced CMR in 26 patients with ischemic cardiomyopathy with mean EF 31±11%. (92) In this setting of patients with chronic ischemic heart disease, the segmental extent of LGE was able to differentiate viable myocardium as defined by PET with a sensitivity of 96% and specificity of 84%. Viability with PET was gauged from segments with either normal or abnormal perfusion based on tetrofosmin uptake as long as there was normal or increased metabolism measured with FDG uptake. This study validated the relationship between myocardial viability and contrast enhanced CMR using metabolic imaging with FDG-PET as an in-vivo standard for viable tissue. In another study comparing viability with contrast-enhanced CMR with PET as the gold standard for imaging scar in 31 patients with chronic ischemic heart disease and mean EF of 28±9%, contrast-enhanced CMR demonstrated a sensitivity of 86% and specificity of 94% for detection of segmental abnormal metabolism on PET. (93) In addition, 55% of subendocardial infarcts detected with contrast-enhanced CMR were considered normal on

PET imaging, likely due to improved spatial resolution with CMR and identification of subendocardial infarction.

In a landmark article in 2002, Kim et al studied 50 patients with LV dysfunction who were evaluated with contrast enhanced CMR prior to surgical or percutaneous revascularization. (94) There was LGE in 80% of the patients with a mean signal intensity of the LGE region that was more than 6 SD greater than normal myocardium. When 12 circumferential segments on short axis images were analyzed, the segments with improved contractility after revascularization were related to the transmural extent of LGE. The mean transmural extent of LGE was 10±7% for dysfunctional segments with improved contractility after revascularization, versus 41±14% for those without improvement ($p<0.001$). In segments with at least severe hypokinesia, a cut off point of 75% transmurality of LGE was found to have 100% negative predictive value for improved contractility with revascularization (Figure 11).

The study by Kim et al (94) demonstrated that close to 80% of myocardial segments with no LGE had functional recovery. However, segments with 1-50% transmural infarction had an uncertain recovery (40-60%). To further evaluate patients prior to revascularization with CABG who had LV dysfunction and a 1-50% transmural infarct seen with LGE, Bove et al studied improvement in resting wall thickening with low dose dobutamine (10 μg/kg/min) and cine CMR imaging to establish areas with inotrophic reserve and thus greater likelihood of functional recovery with surgical revascularization. (95) The degree of transmural enhancement was divided into no LGE, 1-25%, 26-50% or greater than 50% and dysfunctional segments were defined as having wall thickening less than 27% (2 standard deviations lower than normal myocardium). A normal response to dobutamine was an improvement in wall thickening into the normal range. After revascularization with CABG, the improvement in wall thickening was 22±4% for dobutamine responsive segments and 9±4% for non-dobutamine responsive segments ($p<0.03$). For patients with infarct transmurality between 1-50%, the contractile reserve demonstrated by low-dose dobutamine predicted functional recovery after revascularization. In a complementary study by Wellnhofer et al, 29 patients with ischemic cardiomyopathy and severely reduced EF were imaged with low-dose dobutamine during CMR to establish contractile reserve and also underwent LGE imaging to identify the degree of myocardial scar. (96) Based on receiver operator statistics-area under the curve, contractile reserve with low-dose dobutamine was superior to the presence of LGE scar in predicting recovery of LV function, in particular when myocardial segments have LGE less than 75%.

Although evaluating myocardial viability in patients with chronic ischemic heart disease prior to revascularization is focused on improvement in LV systolic function, Samady et al. demonstrated that almost half of all myocardial segments which did not have improvement in resting LV systolic function did have an early improvement in contractile reserve using tagged gradient-echo cine imaging with low dose dobutamine. (97) These segments also appeared to have a late improvement in resting function. In this study, the catheter based technique of LV electromechanical mapping measured regional electrical and mechanical myocardial function as a marker of viability.

3. Evaluating the Etiology of Non-Ischemic Cardiomyopathies

3.a Diagnostic Evaluation

CMR is uniquely capable of answering important questions in the evaluation of cardiomyopathies such as quantification of biventricular volumes and function, underlying etiology and potential modifiable components of the disease process. (98) A comprehensive CMR exam takes advantage of the varied imaging techniques for tissue characterization

with T1 and T2-weighted sequences, cine functional analysis, infarct/fibrosis imaging with LGE and contrast-enhanced myocardial perfusion imaging. The non-ischemic cardiomyopathies with extensive literature supporting an important role for CMR imaging include dilated cardiomyopathy, myocarditis, hypertrophic cardiomyopathy, arrhythmogenic right ventricular cardiomyopathy (ARVC), iron overload cardiomyopathy, amyloidosis, sarcoidosis, and LV non-compaction.

In general, a CMR examination for cardiomyopathy (25) begins with a complete functional assessment of the left and right ventricles using SSFP cine imaging in the 2, 3 and 4 chamber long axis as well as a series of short axis images which cover the entire left ventricle. Using the functional data set, it is possible to quantify EF and ventricular mass and volumes. In the setting of possible myocarditis, T2-weighted imaging is performed prior to contrast administration. Acquiring functional data in other imaging planes is important in certain conditions, such as a stack of sequential axial cine images for better visualization of the right ventricle in cases of suspected ARVC. Acquisition of LGE images are key in differentiating types of cardiomyopathies. The pattern of LGE in non-ischemic cardiomyopathies is in a non-coronary distribution. Typically LGE due to MI occurs in the subendocardial region or has some degree of transmural involvement beginning in the subendocardium and progressing towards the epicardium. In the case of non-ischemic cardiomyopathies, the type of LGE patterns including mid-wall patchy hyperenhancement, epicardial involvement or global subendocardial enhancement (Figure 12), aids in the diagnosis. (11)

The presence of LGE impacts patient prognosis in patients with non-ischemic cardiomyopathies. (99) Wu et al studied a group of 65 patients with EF less than 35% referred for implantable cardiac defibrillator therapy who had no evidence of coronary artery stenosis greater than 50% on X-ray angiogram. The presence of LGE in a non-ischemic distribution likely represents myocardial fibrosis from a variety of pathologies and was predictive of increased cardiac events even after adjusting for EF and heart failure class.

3.b Dilated Cardiomyopathy

CMR using LGE and contrast-enhanced myocardial perfusion with a LV functional assessment is useful in differentiating an ischemic cardiomyopathy with LV cavity dilation and hibernating myocardium from idiopathic dilated cardiomyopathy (DCM). It is not uncommon for patients with DCM to have subendocardial or transmural LGE consistent with prior infarctions, with some estimates as high as 13% of patients. (100) However, these infarctions are either out of proportion to the degree of LV dysfunction or potentially related to vasospasm or embolization. In addition, approximately 16% of DCM patients can have myocardial LGE in the mid-wall in a non-coronary distribution related to myocardial fibrosis. (101) In a study by Soriano et al of 71 patients with a dilated cardiomyopathy and no known history of CAD, findings on CMR with LGE were compared with X-ray angiography in all patients. (102) For the patients without obstructive CAD on angiogram, there were several patterns of LGE: 9% subendocardial or transmural and 9% with mid-wall involvement. Interestingly, 3 patients in the group with obstructive CAD on angiogram also had mid-wall LGE, indicating the co-existence of ischemic and non-ischemic etiologies of the cardiomyopathy. Assomull et al demonstrated the relationship between mid-wall fibrosis in DCM and an increased risk of all-cause death, hospitalization for a cardiovascular event, as well as ventricular tachycardia. (103)

3.c Myocarditis

A recent Journal of the American College of Cardiology White Paper on myocarditis outlines the background of why CMR has become the primary means of non-invasive

evaluation of myocarditis and puts forth consensus diagnostic criteria, the “Lake Louise Criteria.” (104) The CMR examination includes a ventricular functional analysis, as significant myocarditis will often cause a fall in EF. In addition, the presence of a pericardial effusion occurs in a third to half of patients with myocarditis and should be noted as a marker of inflammation. The mainstay of myocarditis evaluation involves tissue characterization with edema seen by T2-weighted images and LGE evaluating for myocardial necrosis or fibrosis. Tissue involvement with myocarditis may be regional or diffuse. Typically the pattern of LGE with myocarditis spares the endocardium and instead involves the mid and epicardium in a patchy or diffuse fashion.

The Lake Louise Criteria state that in the setting of suspected myocarditis, CMR findings are consistent with tissue inflammation if at least two criteria are met: 1) regional or global increase of myocardial SI on T2-weighted images, 2) increased early global myocardial enhancement between myocardium and skeletal muscle on T1-weighted images and 3) at least one focal area of LGE in an non-ischemic pattern. If only criterion three is met, the CMR study is still consistent with myocardial inflammation in the appropriate clinical context. Based on pooled data of 130 patients with either clinical or histologic validation of myocarditis, the diagnostic strategy of using at least two Lake Louise Criteria results in moderate sensitivity of 67% and excellent specificity of 91%.

3.d Hypertrophic Cardiomyopathy

Hypertrophic cardiomyopathy (HCM) is a genetic disorder with abnormal sarcomere proteins resulting in disordered myocytes and fibrosis. (105) Given the varied forms of HCM with asymmetric septal involvement, apical and symmetric hypertrophy, CMR is able to evaluate HCM more completely than other imaging modalities. (106) CMR cine imaging also allows for visualization of associated LV outflow tract obstruction in HCM and systolic anterior motion of the mitral valve with resulting regurgitation.

HCM has a characteristic pattern of LGE with typically patchy and mid-wall involvement, although apical-variant HCM may have apical enhancement. (107) The presence of LGE with HCM correlates with regions of increased deposition of collagen based on histology. (108) Adabag et al performed 24-hour Holter monitor testing and CMR with LGE to evaluate for scar in 71 patients with HCM without significant associated symptoms. (109) The presence of LGE carried a 7-fold increased risk of non-sustained ventricular tachycardia; however, the amount of LGE was not related to arrhythmias.

3.e Arrhythmogenic Right Ventricular Cardiomyopathy

ARVC is a genetic disorder predominantly involving fibro-fatty replacement of the right ventricular (RV) myocardium with resulting dysfunction and enlargement. The diagnosis of ARVC is made by using major and minor criteria determined from clinical, electrophysiologic, histopathologic and imaging data. (110) Morphologic and functional abnormalities of the right ventricle seen with ARVC (Figure 13) and imaged with CMR include the major criteria of localized aneurysms, severe global or segmental dilatation of the right ventricle and global systolic dysfunction while mild dilatation or regional contraction abnormalities of the right ventricle are minor criteria. In order to adequately visualize RV function using CMR, axial and short axis SSFP cine images are obtained as well as long-axis RV views. Patients with ARVC may also have involvement of the left ventricle, although this is less common. (111)

Identifying fibrofatty replacement of the myocardium on T1-weighted images is not part of the diagnostic evaluation since it is the least reproducible parameter. However, finding LGE

in the RV myocardium correlates with fibrofatty infiltration of the myocardium seen on endomyocardial biopsy. (112)

3.f Amyloidosis

The presence of amyloid protein in the myocardial intersititum occurs in about half of patients with amyloidosis and is associated with a characteristic pattern of LGE (Figure 14) with circumferential subendocardial involvement or patchy transmural enhancement due to abnormal gadolinium kinetics with the disrupted myocardial interstitium. (113) The findings on LGE with amyoidosis have been validated against endomyocardial biopsy in 33 patients with diastolic dysfunction and features concerning for amyloid such as unexplained LV hypertrophy. (114) In this group, the typical pattern of circumferential subendocardial LGE had a sensitivity of 80% with biopsy proven amyloid and a specificity of 94%. Maceira et al studied 29 patients with biopsy proven amyloidosis and found LGE in 69% which was uniformly a global, subendocardial pattern. (115)

3.g Sarcoidosis

Sarcoidosis involves the deposition of non-caseating granulomas across multiple organ systems including the heart. CMR can identify characteristic features of cardiac sarcoid including thin septum, ventricular dilation and dysfunction as well as pericardial effusion. There is a diverse pattern of LGE seen with cardiac sarcoid with a classic pattern of mid-wall or epicardial LGE, usually involving the anteroseptal or inferolateral walls. (11) However, the LGE pattern can also include subendocardial or transmural enhancement in any vascular distribution. Smedema et al compared CMR with LGE in 58 patients with biopsy proven pulmonary sarcoid and found 19 patients with evidence of LGE, mostly in the basal and lateral myocardium. (116) In regions of active myocardial inflammation with granulomas, T2-weighted imaging can have regions of increased signal intensity. (117)

3.h Other Non-ischemic Cardiomyopathies

CMR is also able to evaluate a variety of other non-ischemic cardiomyopathies, including (98): transient apical-ballooning syndrome, LV non-compaction with distinct ventricular trabeculations, iron-overload cardiomyopathy seen with beta-thalessemia major or hemochromatosis, Anderson-Fabry disease with abnormal lysosomal metabolism causing hypertrophy and Chagas disease with progressive myocardial fibrosis.

4. Future Directions

CMR imaging in the setting of MI and evaluation of viability with chronic ischemic heart disease provides a robust examination of cardiac function, presence of ischemia, acuity of the infarction, degree of myocardial scar and probability of functional recovery with revascularization. Future developments in the field of CMR will continue to shed light on defining the area at risk in the setting of acute infarctions by exploring advances in T2-weighted imaging. In addition, the potential exists for non-contrast enhanced myocardial perfusion imaging using arterial-spin labeling for patients who are not candidates to receive gadolinium due to co-existing severe renal failure. The future also holds promise for imaging coronary artery atherosclerotic plaque using CMR. (118) At present differentiation of coronary plaque components with CMR is limited by inadequate spatial resolution, however promising research advances are occur in the use of T1-weighted and LGE imaging of coronary arteries. (119) The role of CMR in the evaluation of patients with CAD and congestive heart failure will continue to grow as its utility and prognostic import are further defined.

References

1. Wu K. CMR as the “one-stop shop” for risk stratification after infarction? J Am Coll Cardiol Img 2009;2:843–5.
2. Cerqueira MD, Weissman NJ, Dilsizian V, et al. Standardized myocardial segmentation and nomenclature for tomographic imaging of the heart: a statement for healthcare professionals from the cardiac imaging committee of the council on clinical cardiology of the American Heart Association. Circulation 2002;105:539–542. [PubMed: 11815441]
3. Holman ER, Buller VGM, de Roos A, et al. Detection and quantification of dysfunctional myocardium by magnetic resonance imaging. Circulation 1997;95:924–93. [PubMed: 9054752]
4. Gotte MJW, van Rossum AC, Twisk JWR, et al. Quantification of regional contractile function after infarction: strain analysis superior to wall thickening analysis in discriminating infarct from remote myocardium. J Am Coll Cardiol 2001;37:808–17. [PubMed: 11693756]
5. Bottini PB, Carr AA, Prisant LM, et al. Magnetic resonance imaging compared to echocardiography to assess left ventricular mass in the hypertensive patient. Am J Hypertens 1995;8:221–228. [PubMed: 7794570]
6. Ichikawa Y, Sakuma H, Kitagawa K, et al. Evaluation of left ventricular volumes and ejection fraction using fast steady-state cine MR imaging: comparison with left ventricular angiography. J Cardiovasc Magn Reson 2003;5:333–342. [PubMed: 12765112]
7. Persson E, Carlsson M, Palmer J, et al. Evaluation of left ventricular volumes and ejection fraction by automated gated myocardial SPECT versus cardiovascular magnetic resonance. Clin Physiol Funct Imaging 2005;25:135–141. [PubMed: 15888092]
8. Bellenger NG, Davies LC, Francis JM, et al. Reduction in sample size for studies of remodeling in heart failure by the use of cardiovascular magnetic resonance. J Cardiovasc Magn Reson 2000;2(4): 271–8. [PubMed: 11545126]
9. Nowosielski M, Schocke M, Mayr A, et al. Comparison of wall thickening and ejection fraction by cardiovascular magnetic resonance and echocardiography in acute myocardial infarction. J Cardiovasc Magn Reson 2009;11(1):22. [PubMed: 19589148]
10. Bodi V, Sanchis J, Nunez J, et al. Prognostic value of a comprehensive cardiac magnetic resonance assessment soon after a first ST-segment elevation myocardial infarction. J Am Coll Cardiol Img 2009;2:835–42.
11. Mahrholdt H, Wagner A, Judd RM, Sechtem U, Kim RJ. Delayed enhancement cardiovascular magnetic resonance assessment of non-ischemic cardiomyopathies. Eur Heart J 2005;26:1461–1474. [PubMed: 15831557]
12. Wesbey GE, Higgins CB, McNamara MT, et al. Effect of gadolinium-DTPA on the magnetic relaxation times of normal and infarcted myocardium. Radiology 1984;153:165–169. [PubMed: 6473778]
13. Judd RM, Lugo-Olivieri CH, Arai M, et al. Physiologic basis of myocardial contrast enhancement in fast magnetic resonance images of 2-day-old reperfused canine infarcts. Circulation 1995;92:1902–1910. [PubMed: 7671375]
14. Kim RJ, Fieno DS, Parrish TB, et al. Relationship of MRI delayed contrast enhancement to irreversible injury, infarct age, and contractile dysfunction. Circulation 1999;100:1992–2002. [PubMed: 10556226]
15. Fieno DS, Kim RJ, Chen EL, et al. Contrast-enhanced magnetic resonance imaging of myocardium at risk: distinction between reversible and irreversible injury throughout infarct healing. J Am Coll Cardiol 2000;36:1985–1991. [PubMed: 11092675]
16. de Roos A, van Rossum AC, van der Wall E, et al. Reperfused and non-reperfused myocardial infarction: diagnostic potential of Gd-DTPA enhanced MR imaging. Radiology 1989;172:717–720. [PubMed: 2772179]
17. Lima JAC, Judd RM, Bazille A, et al. Regional Heterogeneity of Human Myocardial Infarcts Demonstrated by Contrast-Enhanced MRI. Circulation 1995;92:1117–1125. [PubMed: 7648655]
18. Simonetti OP, Kim RJ, Fieno DS, et al. An improved MR imaging technique for the visualization of myocardial infarction. Radiology 2001;218:215–223. [PubMed: 11152805]

19. Hundley GW, Narula J. Cardiovascular magnetic resonance imaging: is only one shop worth the stop? J Am Coll Cardiol Img 2009;2(9):1144–1145.
20. Thomson LE, Kim RJ, Judd RM. Magnetic resonance imaging for the assessment of myocardial viability. J Magn Reson Imaging 2004;19:771–788. [PubMed: 15170783]
21. Kellman P, Arai AE, McVeigh ER, Aletras AH. Phase-sensitive inversion recovery for detecting myocardial infarction using gadolinium-delayed hyperenhancement. Magn Reson Med 2002 Feb; 47(2):372–83. [PubMed: 11810682]
22. Sievers B, Elliott MD, Hurwitz LM, et al. Rapid detection of myocardial infarction by subsecond, free-breathing delayed contrast-enhancement cardiovascular magnetic resonance. Circulation 2007;115:236–244. [PubMed: 17200443]
23. Bondarenko O, Beek AM, Hofman MBM, et al. Standardizing the definition of hyperenhancement in the quantitative assessment of infarct size and myocardial viability using delayed contrast-enhanced CMR. J Cardiovas Magn Reson 2005;7(2):481–485.
24. Kramer CM, Barkhausen J, Flamm SD, et al. Standardized cardiovascular magnetic resonance imaging (CMR) protocols, society for cardiovascular magnetic resonance: board of trustees task force on standardized protocols. J Cardiovas Magn Reson 2008;10:35.
25. Hundley WG, Bluemke D, Bogaert JG, et al. Society for cardiovascular magnetic resonance guidelines for reporting cardiovascular magnetic resonance examinations. J Cardiovas Magn Reson 2009;11:5.
26. Choi KM, Kim RJ, Gubernikoff G, et al. Transmural extent of acute myocardial infarction predicts long-term improvement in contractile function. Circulation 2001;104:1101–7. [PubMed: 11535563]
27. Ortiz-Perez JT, Rodriguez J, Meyers SN, Lee DC, Davidson C, Wu E. Correspondence between the 17-segment model and coronary arterial imaging using contrast-enhanced cardiac magnetic resonance imaging. J Am Coll Cardiol Img 2008;1:282–93.
28. Kim RJ, Albert TSE, Wible JH, et al. Performance of delayed-enhancement myocardial resonance imaging with gadoversetamide contrast for the detection and assessment of myocardial infarction. Circulation 2008;117:629–637. [PubMed: 18212288]
29. Wagner A, Mahrholdt H, Thomson L, et al. Effects of time, dose, and inversion time for acute myocardial infarct size measurements based on magnetic resonance imaging-delayed contrast enhancement. J Am Coll Cardiol 2006;47:2027–33. [PubMed: 16697321]
30. Wagner A, Mahrholdt H, Holly TA, et al. Contrast-enhanced MRI and routine single photon emission computed tomography (SPECT) perfusion imaging for detection of subendocardial myocardial infarcts: an imaging study. Lancet 2003 Feb 1;361(9355):374–9. [PubMed: 12573373]
31. Ibrahim T, Bulow HP, Hackl T, et al. Diagnostic value of contrast-enhanced magnetic resonance imaging and single-photon emission computed tomography for detection of myocardial necrosis early after acute myocardial infarction. J Am Coll Cardiol 2007;49:208–216. [PubMed: 17222732]
32. Reimer KA, Jennings RB. The changing anatomic reference base of evolving myocardial infarction. Underestimation of myocardial collateral blood flow and overestimation of experimental anatomic infarct size due to tissue edema, hemorrhage and acute inflammation. Circulation 1979;60:866–876. [PubMed: 476891]
33. Fieno DS, Hillenbrand HB, Rehwald WG, et al. Infarct resorption, compensatory hypertrophy and differing patterns of ventricular remodeling following acute myocardial infarction of varying size. J Am Coll Cardiol 2004;43:2124–2131. [PubMed: 15172424]
34. Ingkanisorn WP, Rhoads KL, Aletras AH, et al. Gadolinium delayed enhancement cardiovascular magnetic resonance correlates with clinical measures of myocardial infarction. J Am Coll Cardiol 2004;43:2253–9. [PubMed: 15193689]
35. Choi CJ, Haji-Momenian S, DiMaria JM, et al. Infarct involution and improved function during healing of acute myocardial infarction: the role of microvascular obstruction. J Cardiovas Magn Reson 2004;6(4):917–925.
36. Lund GK, Stork A, Muellerleile K, et al. Remodeling and analysis of infarct resorption in patients with reperfused myocardial infarcts by using contrast enhanced MR imaging. Radiology 2007;245:95–102. [PubMed: 17885184]

37. Wu E, Ortiz JT, Tejedor P, et al. Infarct size by contrast enhanced cardiac magnetic resonance is a stronger predictor of outcomes than left ventricular ejection fraction or end-systolic volume index: prospective cohort study. Heart 2008;94(6):730–6. [PubMed: 18070953]
38. Tarantini G, Cacciavillani L, Corbetti F, et al. Duration of ischemia is a major determinant of transmurality and severe microvascular obstruction after primary angioplasty: a study performed with contrast-enhanced magnetic resonance. J Am Coll Cardiol 2005;46:1229–1235. [PubMed: 16198836]
39. Kim HW, Klem I, Shah DJ, et al. Unrecognized non-Q-wave myocardial infarction: prevalence and prognostic significance in patients with suspected coronary disease. PLosS Med 2009;6(4):e1000057.
40. Kwong RY, Chan AK, Brown KA, et al. Impact of unrecognized myocardial scar detected by cardiac magnetic resonance imaging on event-free survival in patients presenting with signs or symptoms of coronary artery disease. Circulation 2006;113:2733–2743. [PubMed: 16754804]
41. Kwong RY, Sattar H, Wu H, et al. Incidence and prognostic implication of unrecognized myocardial scar characterized by cardiac magnetic resonance in diabetic patients without clinical evidence of myocardial infarction. Circulation 2008;118:1011–1020. [PubMed: 18725488]
42. Steel K, Broderick R, Gandla V, et al. Complementary prognostic values of stress myocardial perfusion and late gadolinium enhancement imaging by cardiac magnetic resonance in patients with known or suspected coronary artery disease. Circulation 2009;120:1390–1400. [PubMed: 19770399]
43. Schmidt A, Azevedo CF, Cheng A, et al. Infarct tissue heterogeneity by magnetic resonance imaging identifies enhanced cardiac arrhythmia susceptibility in patients with left ventricular dysfunction. Circulation 2007;115:2006–2014. [PubMed: 17389270]
44. Deneke T, Muller KM, Lemke B, et al. Human histopathology of electroanatomic mapping after cooled-tip radiofrequency ablation to treat ventricular tachycardia in remote myocardial infarction. J Cardiovasc Electrophysiol 2005;16:1246–1251. [PubMed: 16302912]
45. Yan AT, Shayne AJ, Brown KA, et al. Contrast-enhanced cardiovascular magnetic resonance imaging is a powerful predictor of post-myocardial infarction mortality. Circulation 2006;114:32–39. [PubMed: 16801462]
46. Roes SD, Borleffs CJW, van der Geest RJ, et al. Infarct tissue heterogeneity assessed with contrast-enhanced MRI predicts spontaneous ventricular arrhythmia in patients with ischemic cardiomyopathy and implantable cardiac defibrillator. CircCardiovasc Imaging 2009;2:183–190.
47. Kribben A, Witzke O, Hillen U, et al. Nephrogenic systemic fibrosis: pathogenesis, diagnosis and therapy. J Am Col Cardiol 2009;53:1621–1628.
48. Niccoli G, Burzotta F, Galiuto L, Crea F. Myocardial no-reflow in humans. J Am Coll Cardiol 2009;54:281–92. [PubMed: 19608025]
49. Reffelmann T, Kloner RA. The “no-reflow” phenomenon: basic science and clinical correlates. Heart 2002;20:39–45.
50. Rogers WJ Jr, Kramer CM, Geskin G, et al. Early contrast-enhanced MRI predicts late functional recovery after reperfused myocardial infarction. Circulation 1999;99:744–750. [PubMed: 9989958]
51. Nijveldt R, Beek AM, Hirsch A, et al. Functional recovery after acute myocardial infarction: comparison between angiography, electrocardiography and cardiovascular magnetic resonance measures of microvascular injury. J Am Coll Cariol 2008;52:181–9.
52. Yan AT, Gibson CM, Larose E, et al. Characterization of microvascular dysfunction after acute myocardial infarction by cardiovascular magnetic resonance first pass perfusion and late gadolinium enhancement imaging. J Cardiovasc Magn Reson 2006;8:831–7. [PubMed: 17060106]
53. Wu KC, Kim RJ, Bleumke DA, et al. Quantification and time course of microvascular obstruction by contrast-enhanced echocardiography and magnetic resonance imaging following acute myocardial infarction and reperfusion. J Am Coll Cardiol 1998;32(6):1756–1764. [PubMed: 9822106]
54. Kwong RY, Schussheim AE, Rekhraj S, et al. Detecting acute coronary syndrome in the emergency department with cardiac magnetic resonance imaging. Circulation 2003;107:531–7. [PubMed: 12566362]

55. Rogers WJ Jr, Kramer CM, Geskin G, et al. Early contrast-enhanced MRI predicts late functional recovery after reperfused myocardial infarction. Circulation 1999;99:744–750. [PubMed: 9989958]
56. Wu KC, Zerhouni EA, Judd RM, et al. Prognostic significance of microvascular obstruction by magnetic resonance imaging in patients with acute myocardial infarction. Circulation 1998;97:765–772. [PubMed: 9498540]
57. Hombach V, Grebe OC, Merkle N, et al. Sequelae of acute myocardial infarction regarding cardiac structure and function and their prognostic significance as assessed by magnetic resonance imaging. Eur Heart J 2005;26:549–557. [PubMed: 15713695]
58. Kramer CM. The prognostic significance of microvascular obstruction after myocardial infarction as defined by cardiac magnetic resonance. Eur Heart J 2005;26:532–533. [PubMed: 15713691]
59. Choi CJ, Haji-Momenian S, DiMaria JM, et al. Infarct involution and improved function during healing of acute myocardial infarction: the role of microvascular obstruction. J Cardiovasc Magn Reson 2004;6(4):917–25. [PubMed: 15646895]
60. Wisenberg G, Prato FS, Carroll SE, et al. Serial nuclear magnetic resonance imaing of acute myocardial infarction with and without reperfusion. Am Heart J 1998;115:510–518. [PubMed: 3344656]
61. Klocke FJ. Emerging applications of T2-weighted cardiac magnetic resonance imaging in acute ischemic syndromes. J Am Coll Cardiol 2009;14(7):1202–1203. [PubMed: 19341861]
62. Aletras AH, Tilak GS, Natanzon A, et al. Retrospective determination of the area at risk for reperfused acute myocardial infarction with T2-weighted cardiac magnetic resonance imaging: histopathologic and displacement encoding with simulated echos (DENSE) functional validations. Circulation 2006;113:1865–70. [PubMed: 16606793]
63. Abdel-Aty H, Zagrosek A, Schulz-Menger J, et al. Delayed enhancement and T2-weighted cardiovascular magnetic resonance imaging differentiate acute from chronic myocardial infarction. Circulation 2004;109:2411–2416. [PubMed: 15123531]
64. Friedrich MG, Abdel-Aty H, Taylor A, Schulz-Menger J, Messroghli D, Dietz R. The salvaged area at risk in reperfused acute myocardial infarction as visualized by cardiovascular magnetic resonance. J Am Coll Cardiol 2008;51:1581–7. [PubMed: 18420102]
65. Carlsson M, Ubachs JFA, Hedstrom E, et al. Myocardium at risk after acute infarction in humans on cardiac magnetic resonance. J Am Coll Cardiol Img 2009;2:569–76.
66. Mikami Y, Sakuma H, Nagata M, et al. Relationship between signal intensity on T2-weighted MR images and presence of microvascular obstruction in patients with acute myocardial infarction. Am J Radiol 2009;193:W321–W326.
67. Cury RC, Shash K, Nagurney JT, et al. Cardiac magnetic resonance with T2-weighted imaging improves detection of patients with acute coronary syndrome in the emergency department. Circulation 2008;118:837–844. [PubMed: 18678772]
68. Kellman P, Aletras AH, Mancini C, McVeigh ER, Arai AE. T2-prepared SSFP improves diagnostic confidence in edema imaging in acute myocardial infarction compared to turbo spin echo. Magn Reson Med 2007;57:891–897. [PubMed: 17457880]
69. Patel AR, Epstein FH, Kramer CK. Evaluation of the microcirculation. J Nuc Cardiol 2008;15:698–708.
70. Barkhausen J, Hunold P, Jochims M, Debatin JF. Imaging of myocardial perfusion with magnetic resonance. J Magn Reson Imaging 2004;19:750–757. [PubMed: 15170781]
71. Gerber BL, Raman SV, Nayak K, et al. Myocardial first-pass perfusion cardiovascular magnetic resonance: history, theory and current state of the art. J Cardiovasc Magn Reson 2008;10:18. [PubMed: 18442372]
72. Schwitter J, Wacker CM, van Rossum AC, et al. MR-Impact: comparison of perfusion-cardiac magnetic resonance with single-photon emission computed tomography for the detection of coronary artery disease in a multicenter, multivendor, randomized trial. Eur Heart J 2008;29:480–489. [PubMed: 18208849]
73. Nandalur KR, Dwamena BA, Choudhri AF, Nadular MR, Carlos RC. Diagnostic performance of stress cardiac magnetic resonance imaging in the detection of coronary artery disease. J Am Coll Cardiol 2007;50:1343–53. [PubMed: 17903634]

74. Klem I, Heitner JF, Shah DJ, et al. Improved detection of coronary artery disease by stress perfusion cardiovascular magnetic resonance with the use of delayed enhancement infarction imaging. J Am Coll Cardiol 2006;47:1630–1638. [PubMed: 16631001]
75. Plein S, Greenwood JP, Ridgway JP, et al. Assessment of non-ST elevation acute coronary syndrome with cardiac magnetic resonance imaging. J Am Coll Cardiol 2004;44:2173–2181. [PubMed: 15582315]
76. Gutberlet M, Noeske R, Schwinge K, Freyhardt P, Felix R, Niendorf T. Comphrensive cardiac magnetic resonance imaging at 3.0 Tesla: feasibility and implications for clinical applications. Invest Radiol 2006;41:154–67. [PubMed: 16428987]
77. Cheng ASH, Pegg TJ, Karamitsos TD, et al. Cardiovascular magnetic resonance perfusion imaging at 3-Tesla for the detection of coronary artery disease. J Am Coll Cardiol 2007;49:2440–9. [PubMed: 17599608]
78. Mollet NR, Dymarkowski S, Volders W, et al. Visualization of ventricular thrombi with contrast-enhanced magnetic resonance imaging in patients with ischemic heart disease. Circulation 2002;106:2873–6. [PubMed: 12460863]
79. Srichai MB, Junor C, Rodriguez LL, Stillman AE, Grimm RA, Lieber ML, et al. Clinical, imaging, and pathological characteristics of left ventricular thrombus: a comparison of contrast-enhanced magnetic resonance imaging, transthoracic echocardiography, and transesophageal echocardiography with surgical or pathological validation. Am Heart J 2006;152(1):75–84. [PubMed: 16824834]
80. Weinsaft JW, Kim HW, Shah DJ, et al. Detection of left ventricular thrombus by delayed-enhancement cardiovascular magnetic resonance: prevalence and markers in patients with systolic dysfunction. J Am Coll Cardiol 2008;52:148–57. [PubMed: 18598895]
81. Assomull RG, Lyne JC, Keenan N, et al. The role of cardiovascular magnetic resonance in patients presenting with chest pain, raised troponin and unobstructed coronary arteries. Eur Heart J 2007;28(10):1242–1249. [PubMed: 17478458]
82. Rahimtoola SH. A perspective on the three large multicenter randomized clinical trials of coronary artery bypass surgery for chronic stable angina. Circulation 1985;72:123–135.
83. Shan K, Constantine G, Sivananthan M, Flamm SD. Role of cardiac magnetic resonance imaging in the assessment of myocardial viability. Circulation 2004;109:1328–1334. [PubMed: 15037539]
84. Allman KC, Shaw LJ, Hachamovitch R, Udelson E. Myocardial viability testing and impact of revascularization on prognosis in patients with coronary artery disease and left ventricular dysfunction: a meta-analysis. J Am Coll Cardiol 2003;39:1151–1158. [PubMed: 11923039]
85. Baer FM, Voth E, Schneider CA, Theissen P, Schicha H, Sechtem U. Comparison of low dose dobutamine gradient echo magnetic resonance imaging and positron emission tomography [18F]fluorodeoxyglucose in patients with chronic coronary artery disease. Circulation 1995;91:1006–1015. [PubMed: 7850935]
86. Baer FM, Voth E, LaRosee K, et al. Comparison of dobutamine transesophageal echocardiography and dobutamine magnetic resonance imaging for detection of residual myocardial viability. Am J Cardiol 1996;78:415–19. [PubMed: 8752185]
87. Nowosielski M, Schocke M, Mayr A, et al. Comparison of wall thickening and ejection fraction by cardiovascular magnetic resonance and echocardiography in acute myocardial infarction. J Card Magn Reson 2009;11:22.
88. Schinkel AFL, Bax JJ, Poldermans D, Elhendy A, Ferrari R, Rahimtoola SH. Hibernating myocardium: diagnosis and patient outcomes. Curr Probl Cardiol 2007;32:375–4100. [PubMed: 17560992]
89. Baer FM, Theissen P, Schneider CA, et al. Dobutamine magnetic resonance imaging predicts contractile recovery of chronically dysfunctional myocardium after successful revascularization. J Am Coll Cardiol 1998;31:1040–1048. [PubMed: 9562005]
90. Geskin G, Kramer CK, Rogers WJ, et al. Quantitative assessment of myocardial viability after infarction by dobutamine magnetic resonance tagging. Circulation 1998;98:217–223. [PubMed: 9697821]
91. Reichek N. MRI myocardial tagging. J Magn Reson Imaging 1999;10:609–16. [PubMed: 10548769]

92. Kuhl HP, Beek AM, van der Weerdt AP, et al. Myocardial viability in chronic ischemic heart diseae: comparison of contrast-enhanced magnetic resonance imaging with (18)F-fluorodeoxyglucose positron emission tomography. J Am Coll Cardiol 2003;41:1341–1348. [PubMed: 12706930]

93. Klein C, Nekolla SG, Bengel FM, et al. Assessment of myocardial viability with contrast-enhanced magnetic resonance imaging: comparison with positron emission tomography. Circulation 2002;105:162–167. [PubMed: 11790695]

94. Kim RJ, Wu E, Rafael A, et al. The use of contrast-enhanced magnetic resonance imaging to identify reversible myocardial dysfunction. N Engl J Med 2000;343:1445–53. [PubMed: 11078769]

95. Bove CM, DiMaria JM, Voros S, Conaway MR, Kramer CM. Dobutamine response and myocardial infarct transmurality: functional improvement after coronary artery bypass grafting – initial experience. Radiology 2006;240:835–841. [PubMed: 16926330]

96. Wellnhofer E, Olariu A, Klein C, et al. Magnetic resonance low-dose dobutamine test is superior to scar quantification for prediction of functional recovery. Circulation 2004;109:2172–2174. [PubMed: 15117834]

97. Samady H, Choi CJ, Ragosta M, et al. Electromechanical mapping identifies improvement in function and retention of contractile reserve after revascularization in ischemic cardiomyopathy. Circulation 2004;110:2410–2416. [PubMed: 15477418]

98. Karamitos TD, Francis JM, Myerson S, et al. The role of cardiovascular magnetic resonance imaging in heart failure. J Am Coll Cardiol 2009;54:1407–24. [PubMed: 19796734]

99. Wu KC, Weiss RG, Thiemann DR, et al. Late gadolinium enhancement by cardiovascular magnetic resonance heralds an adverse prognosis in non-ischemic cardiomyopathy. J Am Coll Cardiol 2008;51:2414–21. [PubMed: 18565399]

100. McCrohon JA, Moon JC, Prasad SK, et al. Differentiation of heart failure related to dilated cardiomyopathy and coronary artery disease using gadolinium-enhanced cardiovascular magnetic resonance. Circulation 2003;108:54–9. [PubMed: 12821550]

101. Casolo G, Minneci S, Manta R, et al. Identification of the ischemic etiology of heart failure by cardiovascular magnetic resonance imaging: diagnostic accuracy of late gadolinium enhancement. Am Heart J 2006;151:101–8. [PubMed: 16368300]

102. Soriano CJ, Ridocci F, Estornell J, et al. Noninvasive diagnosis of coronary artery disease in patients with heart failure and systolic dysfunction of uncertain etiology, using late gadolinium-enhanced cardiovascular magnetic resonance. J Am Coll Cardiol 2005;45:743–8. [PubMed: 15734620]

103. Assomull RG, Prasad SK, Lyne J, Smith G, Burman ED, Khan M, et al. Cardiovascular magnetic resonance, fibrosis, and prognosis in dilated cardiomyopathy. J Am Coll Cardiol 2006 Nov 21;48(10):1977–85. [PubMed: 17112987]

104. Friedrich MG, Sechtem U, Schulz-Menger J, et al. Cardiovascular magnetic resonance in myocarditis: a JACC white paper. J Am Coll Cardiol 2009;53(17):1475–1487. [PubMed: 19389557]

105. Maron BJ. Hypertrophic cardiomyopathy: a systematic review. JAMA 2002 Mar 13;287(10): 1308–20. [PubMed: 11886323]

106. Rickers C, Wilke NM, Jerosch-Herold M, et al. Utility of cardiac magnetic resonance imaging in the diagnosis of hypertrophic cardiomyopathy. Circulation 2005;112:855–61. [PubMed: 16087809]

107. Rudolph A, Abdel-Aty H, Bohl S, et al. Noninvasive detection of fibrosis applying cardiovascular magnetic resonance in different forms of left ventricular hypertrophy relation to remodeling. J Am Coll Cardiol 2009;53:284–91. [PubMed: 19147047]

108. Moon JC, Reed E, Sheppard MN, et al. The histologic basis of late gadolinium enhancement cardiovascular magnetic resonance in hypertrophic cardiomyopathy. J Am Coll Cardiol 2004;43:2260–4. [PubMed: 15193690]

109. Adabag SA, Maron BJ, Appelbaum E, et al. Occurence and frequency of arrhythmias in hypertrophic cardiomyopathy in relation to delayed enhancement on cardiovascular magnetic resonance. J Am Coll Cardiol 2008;51:1369–74. [PubMed: 18387438]

110. McKenna WJ, Thiene G, Nava A, et al. Diagnosis of arrhythmogenic right ventricular dysplasia/cardiomyopathy. Br Heart J 1994;71(3):215–218. [PubMed: 8142187]

111. Corrado D, Basso C, Thiene G, et al. Spectrum of clinicopathologic manifestations of arrhythmogenic right ventricular cardiomyopathy/dysplasia: a multi-center study. J Am Coll Cardiol 1997;30:1512–20. [PubMed: 9362410]

112. Tandri H, Bomma C, Calkins H, Bluemke DA. Magnetic resonance and computed tomography imaging of arrhythmogenic right ventricular dysplasia. J Magn REson Imaging 2004;19:848–58. [PubMed: 15170788]

113. Selvanayagam JB, Hawkins PN, Paul B, et al. Evaluation and management of the cardiac amyloidosis. J Am Coll Cardiol 2007;50:2101–10. [PubMed: 18036445]

114. Vogelsberg H, Mahrholdt H, Deluigi CC, et al. Cardiovascular magnetic resonance in clinically suspected cardiac amyloidosis: noninvasive imaging compared to endomyocardial biopsy. J Am Coll Cardiol 2008;51:1022–30. [PubMed: 18325442]

115. Maceira AM, Joshi J, Prasad SK, et al. Cardiovascular magnetic resonance in cardiac amyloidosis. Circulation 2005;111:186–193. [PubMed: 15630027]

116. Smedema JP, Snoep G, van Kroonenburgh MPG, et al. Evaluation of the accuracy of gadolinium-enhanced cardiovascular magnetic resonance in the diagnosis of cardiac sarcoidosis. J Am Coll Cardiol 2005;45:1683–90. [PubMed: 15893188]

117. Vignaux O, Dhote R, Duboc D, et al. Detection of myocardial involvement in patients with sarcoidosis applying T2-weighted, contrast-enhanced, and cine magnetic resonance imaging: initial results of a prospective study. J Comput Assist Tomogr 2002;26(5):762–7. [PubMed: 12439312]

118. Kramer CM, Narula J. Atherosclerotic plaque imaging: the last frontier for cardiac magnetic resonance. J Am Coll Cardiol Img 2009;2:916–918.

119. Kawasaki T, Koga S, Koga N, et al. Characterization of hyperintense plaque with non-contrast T1-weighted cardiac magnetic resonance coronary plaque imaging: comparison with multi-slice computed tomography and intravascular ultrasound. J Am Coll Cardiol Img 2009;2:720–728.

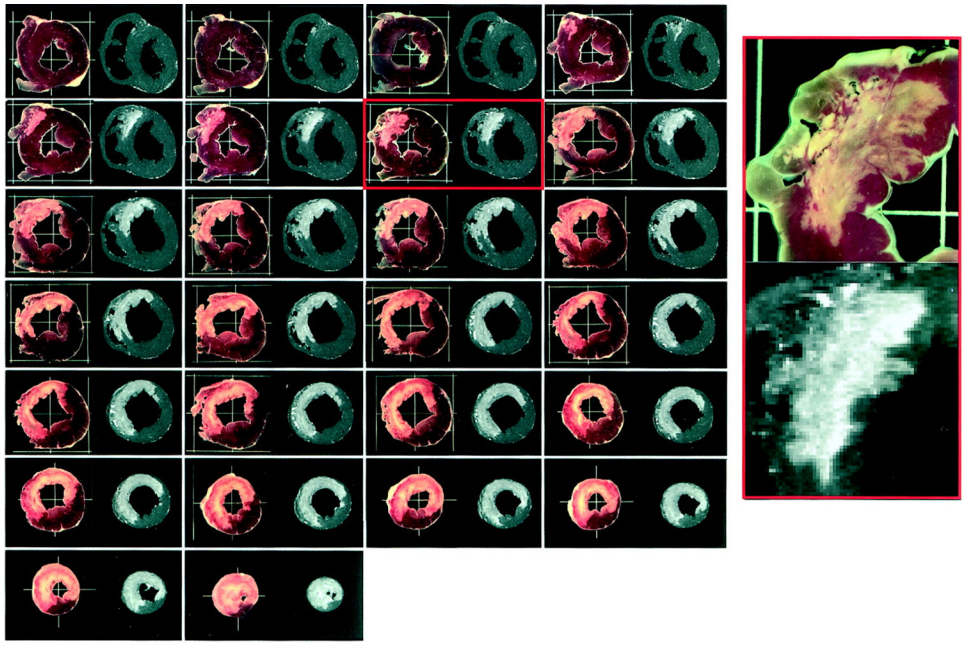

Figure 1.
A comparison of sequential short axis ex vivo views of a canine heart with areas of necrosis seen with triphenyltetrazolium chloride (TTC) (column left) compared late gadolinium enhancement (LGE) magnetic resonance images (column right). Note the excellent correlation between myocardial necrosis seen with TTC and the presence of scar using LGE imaging. Reproduced with permission from: Kim RJ, Fieno DS, Parrish TB, et al. Relationship of MRI delayed contrast enhancement to irreversible injury, infarct age, and contractile dysfunction. Circulation 1999;100:1992-2002.

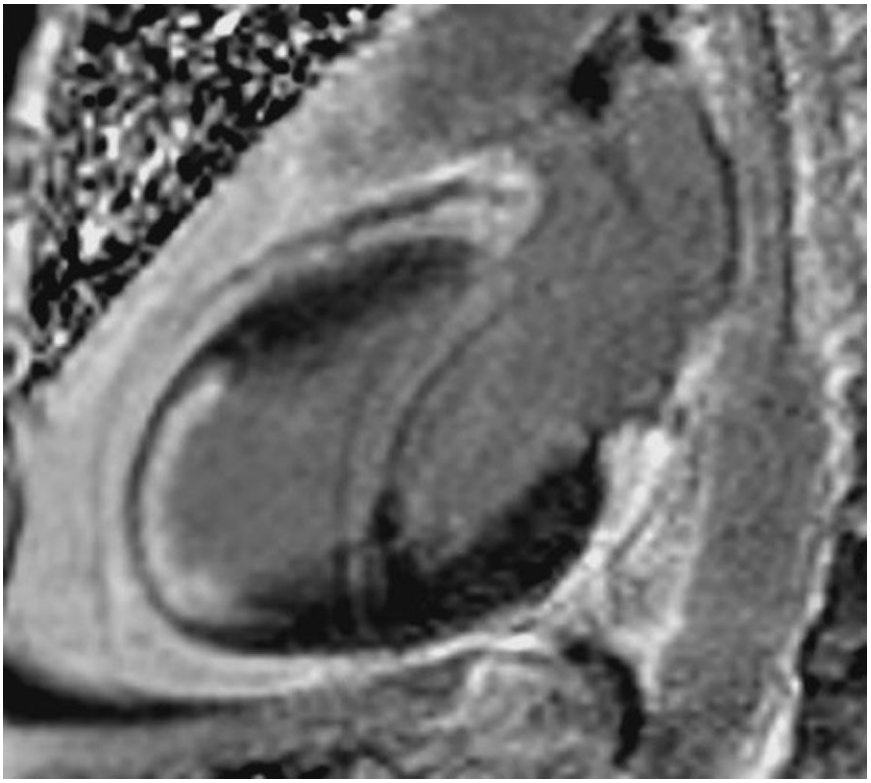

Figure 2.
Patient with history of remote anterior infarction and X-ray angiography with chronically occluded left anterior descending artery. The two-chamber CMR image demonstrated more than 75% transmural LGE (white) involving the anterior and anteroapical wall.

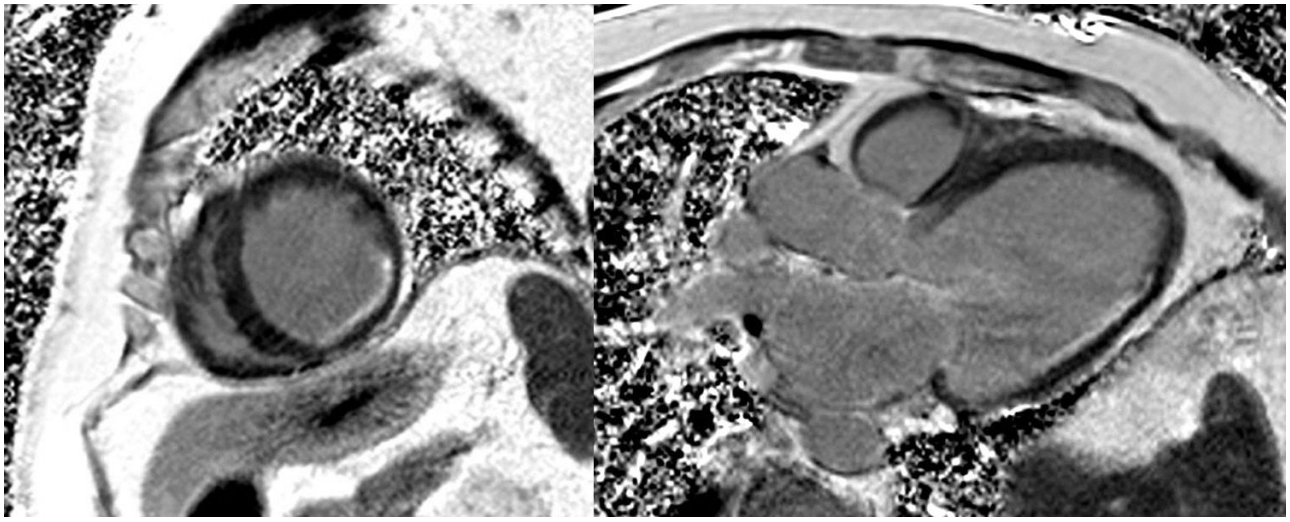

Figure 3.
80 year old patient with known multi-vessel CAD and severely reduced EF. There is dilation of the left ventricle and LGE of the posterolateral wall in the mid ventricle seen on the short axis image (left) and three chamber (right) with less than 25% transmural involvement indicating substantial viability.

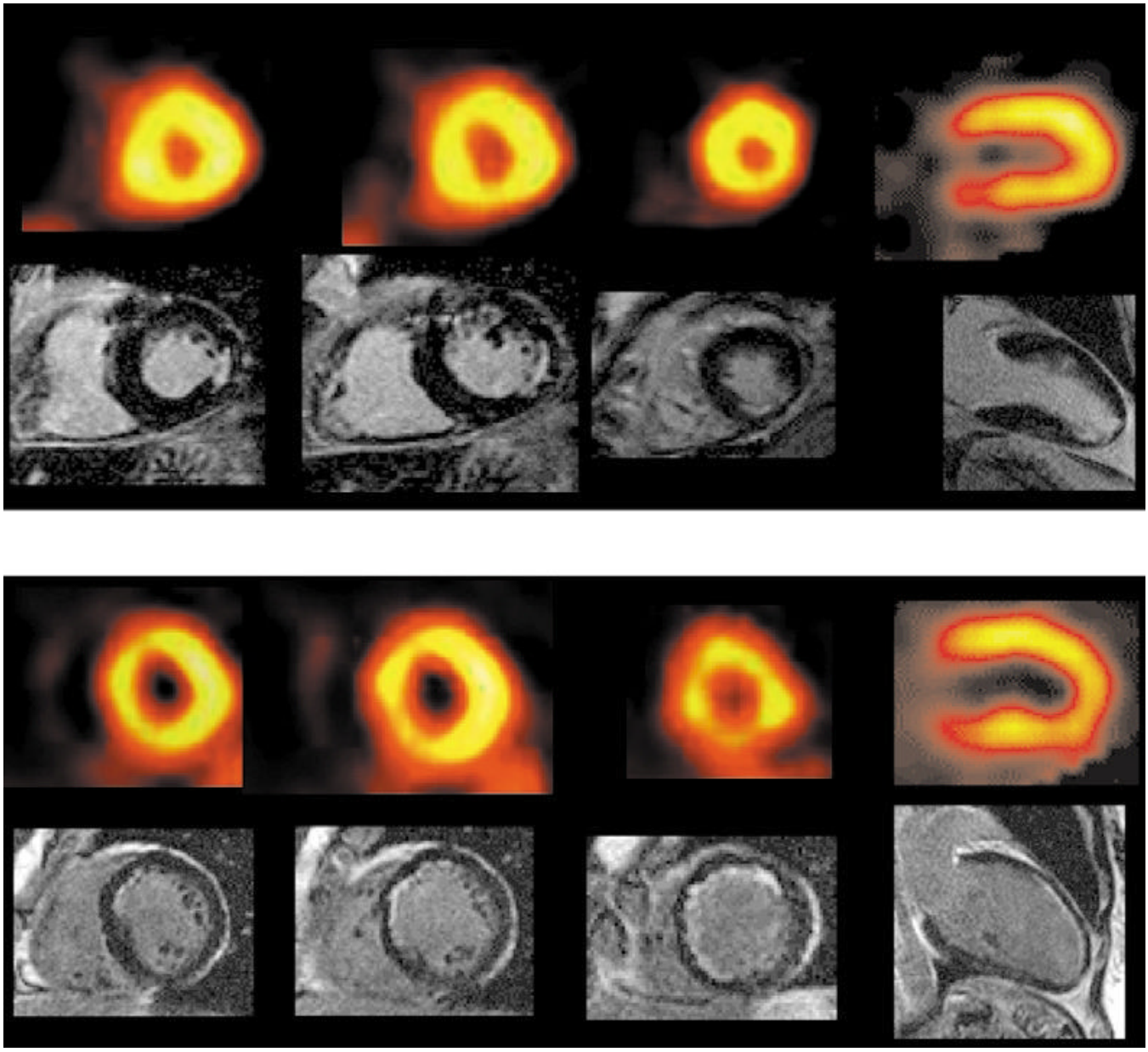

Figure 4.
Normal SPECT images (top row in each panel) in two patients compared to corresponding CMR images demonstrating subendocardial infarcts using LGE imaging. Reprinted from The Lancet 361, Wagner A, Mahrholdt H, Holly TA, et al. Contrast-enhanced MRI and routine single photon emission computed tomography (SPECT) perfusion imaging for detection of subendocardial myocardial infarcts: an imaging study, pages 374-9, 2003, with permission from Elsevier.

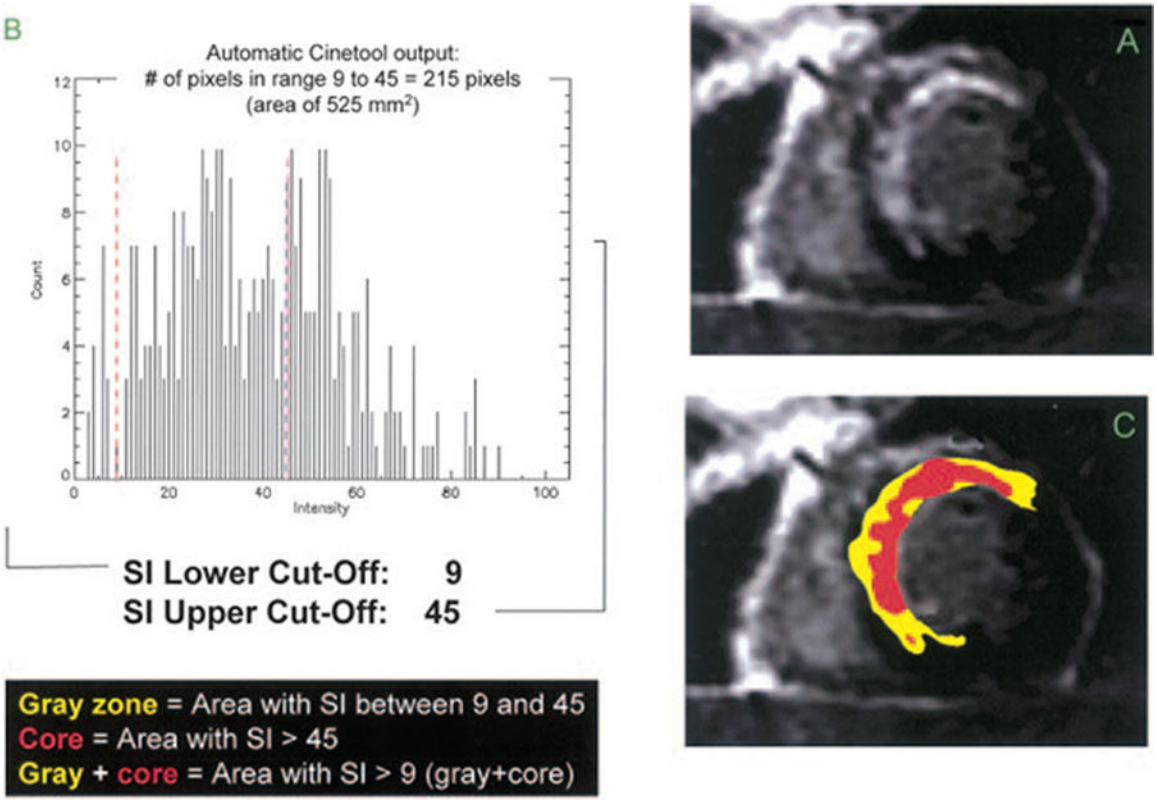

Figure 5.

A short axis late gadolinium enhancement (LGE) image from a patient with anterior infarction (panel A) where the extent of the gray zone was calculated as the area with signal intensity (SI) between maximum SI from normal remote myocardium and 50% of maximum LGE SI and is highlighted in yellow (panel C). In this example, the peak SI in normal remote myocardium is 9, therefore abnormal enhancement was considered in areas with SI greater than 9. A histogram of SI in the region of LGE (panel B) shows a maximum SI of 90, so that the upper limit of SI for the gray area is 50% of 90, or 45. The core area of LGE is highlighted in red (panel C) and is defined as the area with SI greater than 50% of maximum. In this example, the core area of LGE has a SI greater than 45. Reproduced with permission from Schmidt A, Azevedo CF, Cheng A, et al. Infarct tissue heterogeneity by magnetic resonance imaging identifies enhanced cardiac arrhythmia susceptibility in patients with left ventricular dysfunction. Circulation. 2007;115:2006-2014.

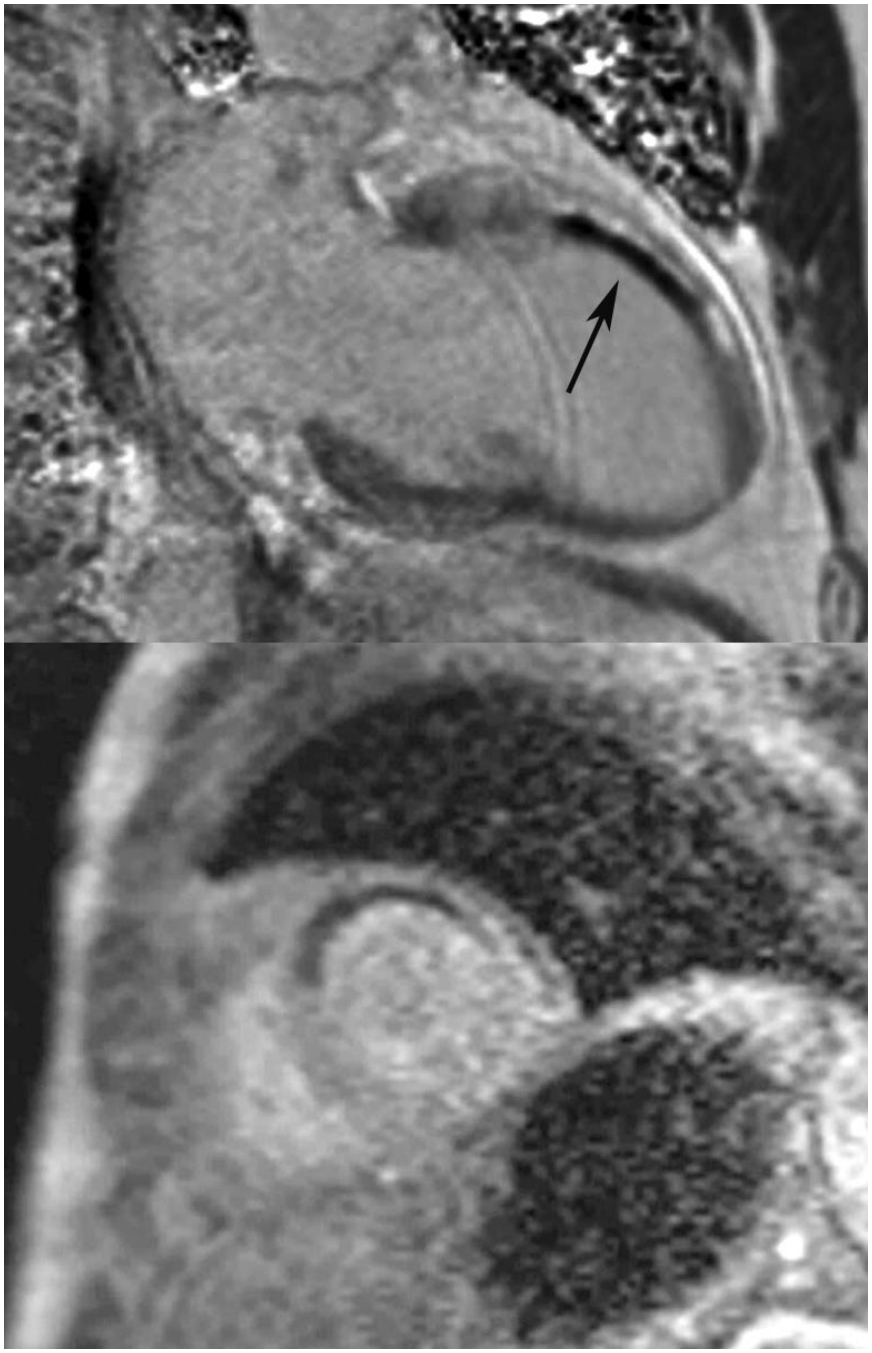

Figure 6.
Phase sensitive inversion recovery gradient echo two chamber image (top) of a patient with evidence of microvascular obstruction (black, see arrow) in the mid anterior wall subendocardium surrounded by late gadolinium enhancement (bright signal) due to a non-ST elevation myocardial infarction from occlusion of the first diagonal artery. Note the resting hypoperfusion in the anteroseptum on first-pass contrast enhanced perfusion imaging on the corresponding mid-ventricle short axis image (bottom).

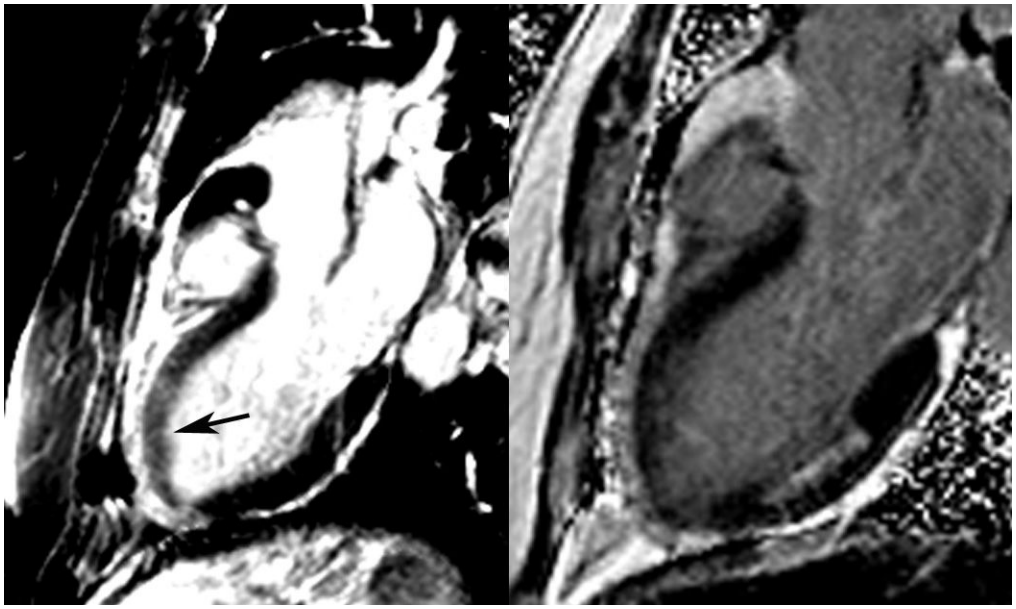

Figure 7.

Patient presenting with chest pain and increased signal intensity on T2-weighted two chamber image (left) consistent with myocardial edema in the anterior wall (arrow). Using late gadolinium enhancement (right), an unrelated subendocardial posterior infarction was seen, however there was no evidence of anterior infarction. Functional imaging of the left ventricle at that time demonstrated an anterior wall motion abnormality due to myocardial ischemic stunning which ultimately resolved.

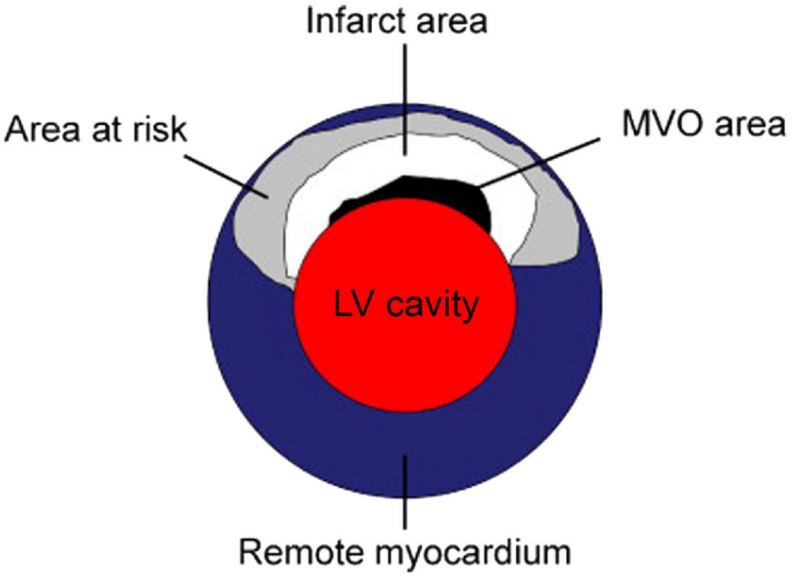

Figure 8.
This illustration demonstrates the area of infarction, defined by both late gadolinium enhancement (white) and microvascular obstruction (black) surrounded by the area at risk (gray) which represents the potential area of myocardial salvage. Reprinted from Journal of the American College of Cardiology: Cardiovascular Imaging, volume 2, Mather AN, Greenwood JP and Plein S. Characterization of acute myocardial infarction by magnetic resonance imaging, pages 1141-1143, 2009, with permission from Elsevier.

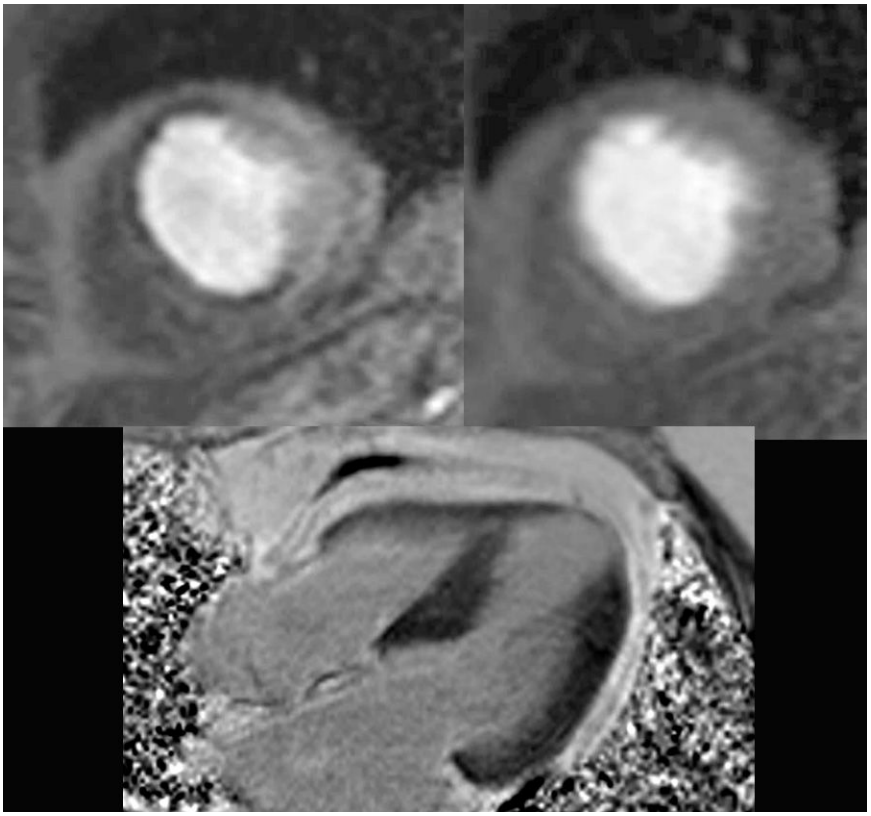

Figure 9.
Stress perfusion cardiac magnetic resonance (CMR) imaging obtained after 3 minutes of adenosine demonstrating hypoperfusion to the anterior and anteroseptal walls (top left), followed by normal rest perfusion imaging 10 minutes later (top right). The 4 chamber view late gadolinium enhancement image demonstrates a thin apex and no enhancement (lower left). The stress perfusion CMR thus demonstrated ischemia and at cardiac catheterization the patient had three vessel disease involving his ramus, first obtuse-maginal and left anterior descending.

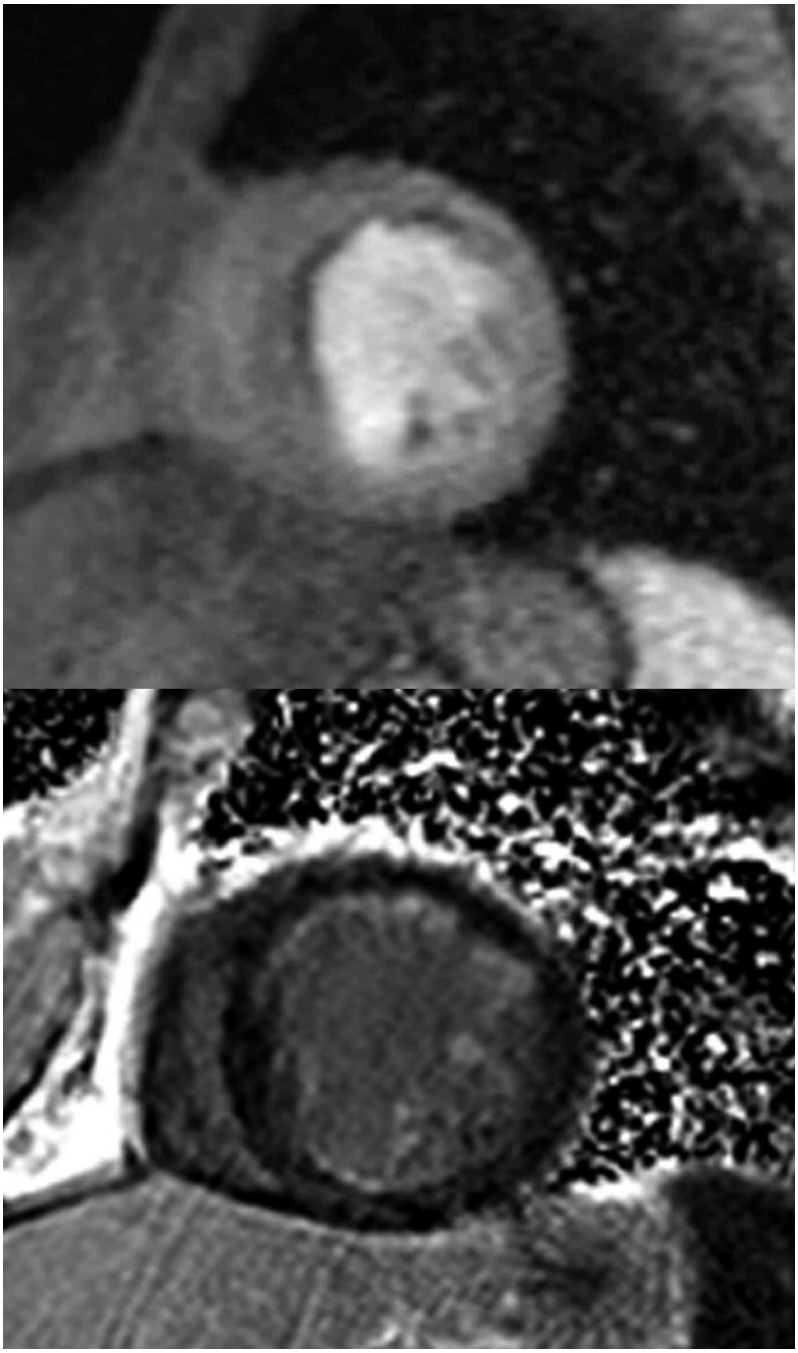

Figure 10.
A 57 year old with an anterior and anteroseptal resting perfusion abnormality seen on a basal short axis image (top image) and evidence of less than 25% subendocardial late gadolinium enhancement (bottom image) involving the anterior, inferior and septum indicating predominantly viable myocardium in a patient with multi-vessel CAD and a reduced ejection fraction.

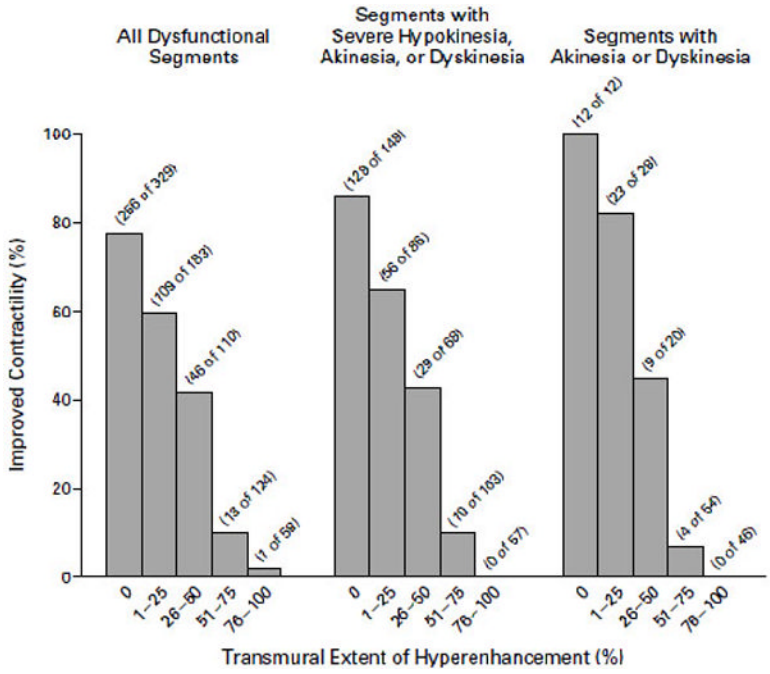

Figure 11.

The relationship between transmural extent of late gadolinium enhancement, dysfunctional myocardium segments and improved contractility with revascularization. Reproduced with permission from Kim RJ, Wu E, Rafael A, et al. The use of contrast-enhanced magnetic resonance imaging to identify reversible myocardial dysfunction. New England Journal of Medicine 2000;343:1445-53. Copyright © 2000 *Massachusetts Medical Society. All rights reserved.*

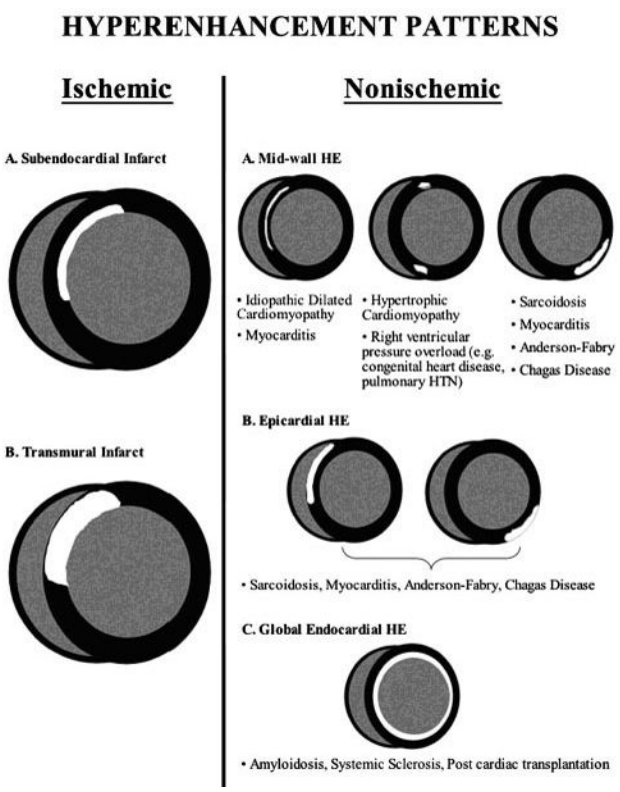

Figure 12.

Patterns of late gadolinium enhancement seen in ischemic and non-ischemic cardiomyopathies. Mahrholdt H, Wagner A, Judd RM, Sechtem U, Kim RJ. Delayed enhancement cardiovascular magnetic resonance assessment of non-ischemic cardiomyopathies. European Heart Journal 2005;26:1461-1474, European Society of Cardiology, by permission of Oxford University Press.

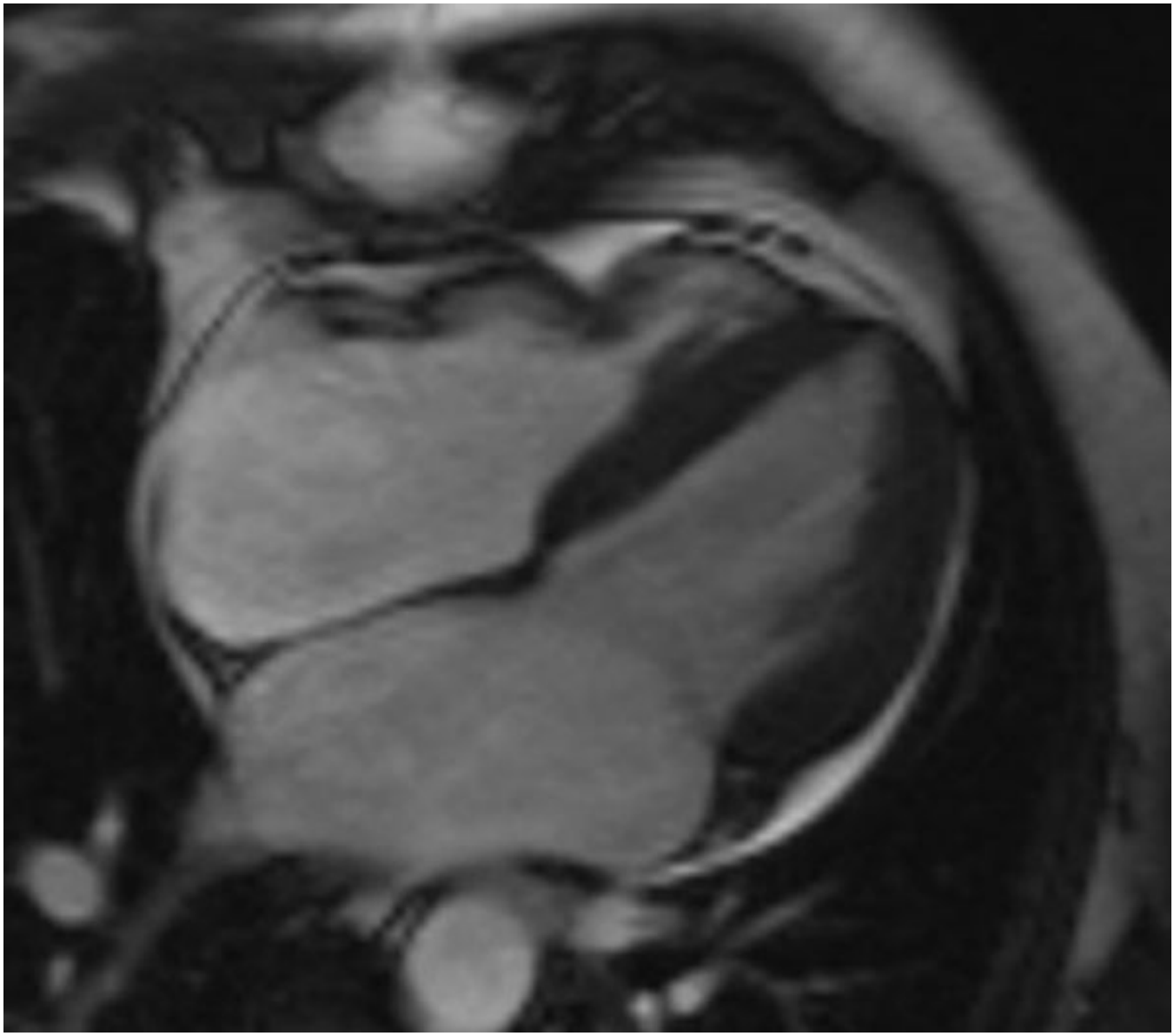

Figure 13.
A patient with focal regional dysfunction of the anterior right ventricle consistent with arrhythmogenic right ventricular cardiomyopathy seen on this single end-systolic steady-state free precession image.

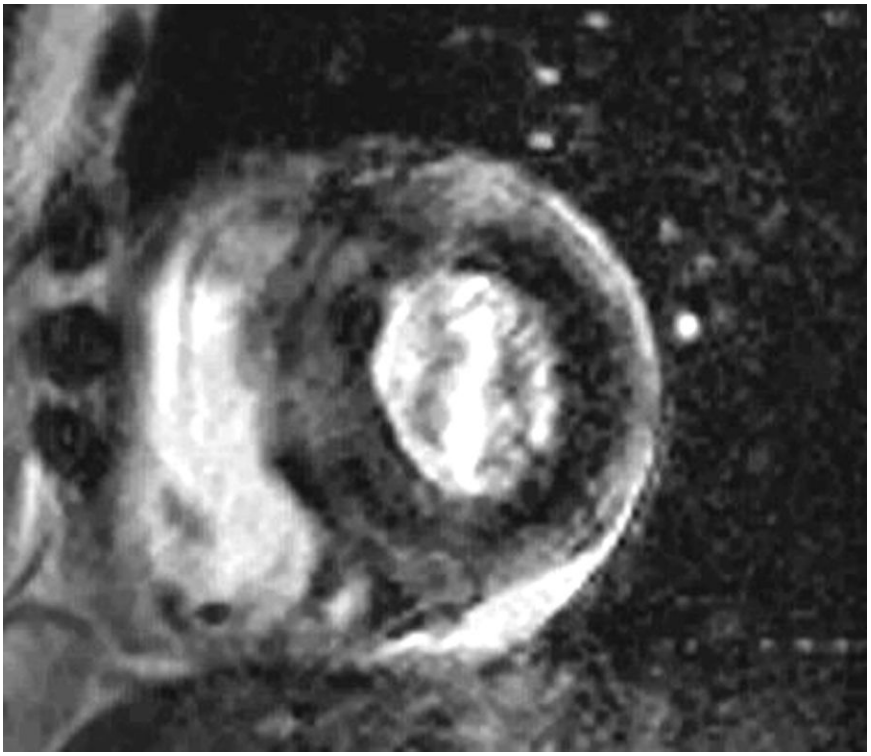

Figure 14.
A patient with known amyloidosis referred for cardiac magnetic resonance imaging due to heart failure with preserved systolic function and concern for infiltrative cardiomyopathy. The late gadolinium enhanced images demonstrated diffuse patchy enhancement in a non-coronary distribution consistent with cardiac amyloid.